Allegol Int. 2010 in press.
5) Takabayashi T, Xie MJ, Takeuchi S, Kawasaki M, Yagi H, Okamoto M, Tariqur RM, Malik F, Kuroda K, Kubota C, Fujieda S, Nagano T, Sato M.: LL5beta directs the translocation of filamin A and SHIP2 to sites of phosphatidylinositol 3,4,5-triphosphate (PtdIns(3,4,5)P3) accumulation, and PtdIns(3,4,5)P3 localization is mutually modified by co-recruited SHIP2. J Biol Chem. 2010:285:16155-65.
6) Imoto Y, Enomoto H, Fujieda S, Okamoto M, Sakashita M, Susuki D, Okada M, Hirota T, Tamari M, Ebe K, Arinami T, Noguchi E.: S2554X mutation in the filaggrin gene is associated with allergen sensitization in the Japanese population. J Allergy Clin Immunol. 2010, 125:498-500.
7) Yamada T, Lizhong S, Takahashi N, Kubo S, Narita N, Suzuki D, Takabayashi T, Kimura Y, Fujieda S.: Poly(I:C) induces BLyS-expression of airway fibroblasts through phosphatidylinositol 3-kinase. Cytokine. 2010, 50:163-9.
8) Sakashita M, Hirota T, Harada M, Nakamichi R, Tsunoda T, Osawa Y, Kojima A, Okamoto M, Suzuki D, Kubo S, Imoto Y, Nakamura Y, Tamari M, Fujieda S.: Prevalence of allergic rhinitis sensitization to common aeroallergens in a Japanese population. Int Arch Allergy Immunol. 2010, 151:255-61.
9) Kimura Y, Sugimoto C, Takabayashi T, Tanaka T, Kojima A, Narita N, Fujieda S.: Bax-gene transfer enhances apoptosis by steroid treatment in human nasal fibroblasts. Eur Arch Otorhinolaryngol. 2010, 267:61-6.
10) 藤枝重治:スギ花粉症の病状把握と克服に向けて. 第 60 回日本アレルギー学会秋季学術大会 2010.11.
11) 坂下雅文、広田朝光、富田かおり、扇和弘、伊藤有未、岡本昌之、大澤陽子、山田武千代、玉利真由美、藤枝重治:小児気管支喘息関連領域 17q21 の SNPs とアレルギー性鼻炎との関連解析. 第 60 回日本アレルギー学会秋季学術大会 2010.11.
12) 意元義政、野口恵美子、有波忠雄、藤枝重治:網羅的遺伝子解析によるスギ花粉症発症に関する遺伝子同定. 第 60 回日本アレルギー学会秋季学術大会 2010.11.
13) 野口恵美子、藤枝重治:アレルギー疾患のプロオテオミクス. 第 60 回日本アレルギー学会秋季学術大会 2010.11.

H. 知的財産権の出願・登録状況(予定を含む)

1. 特許取得
   なし
2. 実用新案登録
   なし
3. その他
   なし

THE JOURNAL OF BIOLOGICAL CHEMISTRY VOL. 285, NO. 21, pp. 16155–16165, May 21, 2010

LL5β Directs the Translocation of Filamin A and SHIP2 to Sites of Phosphatidylinositol 3,4,5-Triphosphate (PtdIns(3,4,5)P_3) Accumulation, and PtdIns(3,4,5)P_3 Localization Is Mutually Modified by Co-recruited SHIP2*[S]

Received for publication, November 5, 2009, and in revised form, February 2, 2010 Published, JBC Papers in Press, March 17, 2010, DOI 10.1074/jbc.M109.081901

Tetsuji Takabayashi[‡§1], Min-Jue Xie[‡¶1], Seiji Takeuchi[‡¶2], Motomi Kawasaki[‡], Hideshi Yagi[‡¶], Masayuki Okamoto[‡§], Rahman M. Tariqur[‡3], Fawzia Malik[‡], Kazuki Kuroda[‡¶], Chikara Kubota[‡‖], Shigeharu Fujieda[§], Takashi Nagano[‡4], and Makoto Sato[‡¶5]

From the [‡]Division of Cell Biology and Neuroscience, Department of Morphological and Physiological Sciences, the [§]Division of Otorhinolaryngology Head and Neck Surgery, Department of Sensory and Locomotor Medicine, the [‖]Division of Orthopedic Surgery and Rehabilitation Medicine, Department of Surgery, Faculty of Medical Sciences, and the [¶]Research and Education Program for Life Science, University of Fukui, Fukui 910-1193, Japan

Phosphatidylinositol 3,4,5-triphosphate (PtdIns(3,4,5)P_3) accumulates at the leading edge of migrating cells and works, at least partially, as both a compass to indicate directionality and a hub for subsequent intracellular events. However, how PtdIns(3,4,5)P_3 regulates the migratory machinery has not been fully elucidated. Here, we demonstrate a novel mechanism for efficient lamellipodium formation that depends on PtdIns(3,4,5)P_3 and the reciprocal regulation of PtdIns(3,4,5)P_3 itself. LL5β, whose subcellular localization is directed by membrane PtdIns(3,4,5)P_3, recruits the actin-cross-linking protein Filamin A to the plasma membrane, where PtdIns(3,4,5)P_3 accumulates, with the Filamin A-binding Src homology 2 domain-containing inositol polyphosphate 5-phosphatase 2 (SHIP2). A large and dynamic lamellipodium was formed in the presence of Filamin A and LL5β by the application of epidermal growth factor. Conversely, depletion of either Filamin A or LL5β or the overexpression of either an F-actin-cross-linking mutant of Filamin A or a mutant of LL5β without its PtdIns(3,4,5)P_3-interacting region inhibited such events in COS-7 cells. Because F-actin initially polymerizes near the plasma membrane, it is likely that membrane-recruited Filamin A efficiently cross-links newly polymerized F-actin, leading to enhanced lamellipodium formation at the site of PtdIns(3,4,5)P_3 accumulation. Moreover, we demonstrate that co-recruited SHIP2 dephosphorylates PtdIns(3,4,5)P_3 at the same location.

Directed migration is crucial in many biological events, including morphogenesis during development, accumulation of immune cells to the site of infection, and metastasis of cancer cells. A lamellipodium (a sheet-like process composed of actin filaments) must be formed correctly at the leading edge of a cell for smooth and efficient migration. Following stimulation with a chemoattractant, phosphatidylinositol 3-kinase (PI3K)[6] is locally activated, resulting in the transient accumulation of PtdIns(3,4,5)P_3 on the leading edge of directed migrating amoebas and leukocytes (1). PtdIns(3,4,5)P_3 works, at least in part, as a cell compass that translates external signals into directed cell movement (2). However, how PtdIns(3,4,5)P_3 contributes to the appropriate formation of a lamellipodium, or conversely, how lamellipodium formation influences PtdIns(3,4,5)P_3 accumulation has not been fully elucidated. For proper lamellipodium formation, the intracellular network of actin filaments (F-actins) must be regulated both dynamically and precisely. Such networks are composed primarily of cross-linked and branched F-actins. Previous work has shown that Filamin A cross-links F-actins and is indispensable for lamellipodium formation, whereas the Wiskott-Aldrich syndrome protein family verprolin homologous (WAVE) proteins are involved in branch formation (3–5).

Proteins involved in signal transduction and cytoskeletal dynamics interact with membrane phosphoinositides through their pleckstrin homology (PH) domains; such interactions

* This work was supported in part by grants from the 21st Century Center of Excellence program (Biomedical Imaging Technology Integration Program), the Project Allocation Fund of the University of Fukui, the Toray Science Foundation, and the Ministry of Education, Culture, Sports, Science and Technology of Japan.

[S] The on-line version of this article (available at http://www.jbc.org) contains supplemental Experimental Procedures, Figs. S1–S7, and Videos 1–4.

[1] Both authors contributed equally to this work.
[2] Present address: Dept. of Dermatology, Kobe University Graduate School of Medicine, 7-5-1 Kusunoki, Kobe, Hyogo 650-0017, Japan.
[3] Present address: Dept. of Biomedical Science, Kulliyyah of Science, International Islamic University Malaysia, P. O. Box 141, 25710 Kuantan, Pahang Darul Makmur, Malaysia.
[4] Present address: Laboratory of Chromatin and Gene Expression, The Babraham Institute, Cambridge CB22 3AT, United Kingdom.
[5] To whom correspondence should be addressed: 23 Matsuokashimoaizuki, Eiheiji, Fukui 910-1193, Japan. Tel.: 81-776-61-8305; Fax: 81-776-61-8155; E-mail: makosato@u-fukui.ac.jp.

[6] The abbreviations used are: PI3K, phosphatidylinositol 3-kinase; PtdIns, phosphatidylinositol; PtdIns(3,4,5)P_3, phosphatidylinositol 3,4,5-triphosphate; ABD, actin-binding domain of Filamin A; ARNO, ARF nucleotide-binding site opener; PH, pleckstrin homology; FR, filamin repeats; COS-7, African green monkey SV40-transfected kidney fibroblast cell line; EGF, epidermal growth factor; GFP, green fluorescent protein; EGFP, enhanced green fluorescent protein; F-actin, actin filament; HA, hemagglutinin; SHIP2, Src homology 2 domain-containing inositol polyphosphate 5-phosphatase 2; MALDI-TOF, matrix-assisted laser desorption ionization/time of flight; RNAi, RNA interference; shRNA, short hairpin RNA; VSV, vesicular stomatitis virus.

are critical for the subcellular localization of these proteins and the regulation of their activities (6, 7). Although the core tertiary structure is conserved among PH domains, high sequence variability among their primary structures (~120 amino acids) gives rise to different specificities of PH domains for different phosphoinositides (8, 9). LL5β (PHLDB2; pleckstrin homology-like domain, family B, member 2) is an ~160-kDa protein that contains two predicted coiled-coil domains

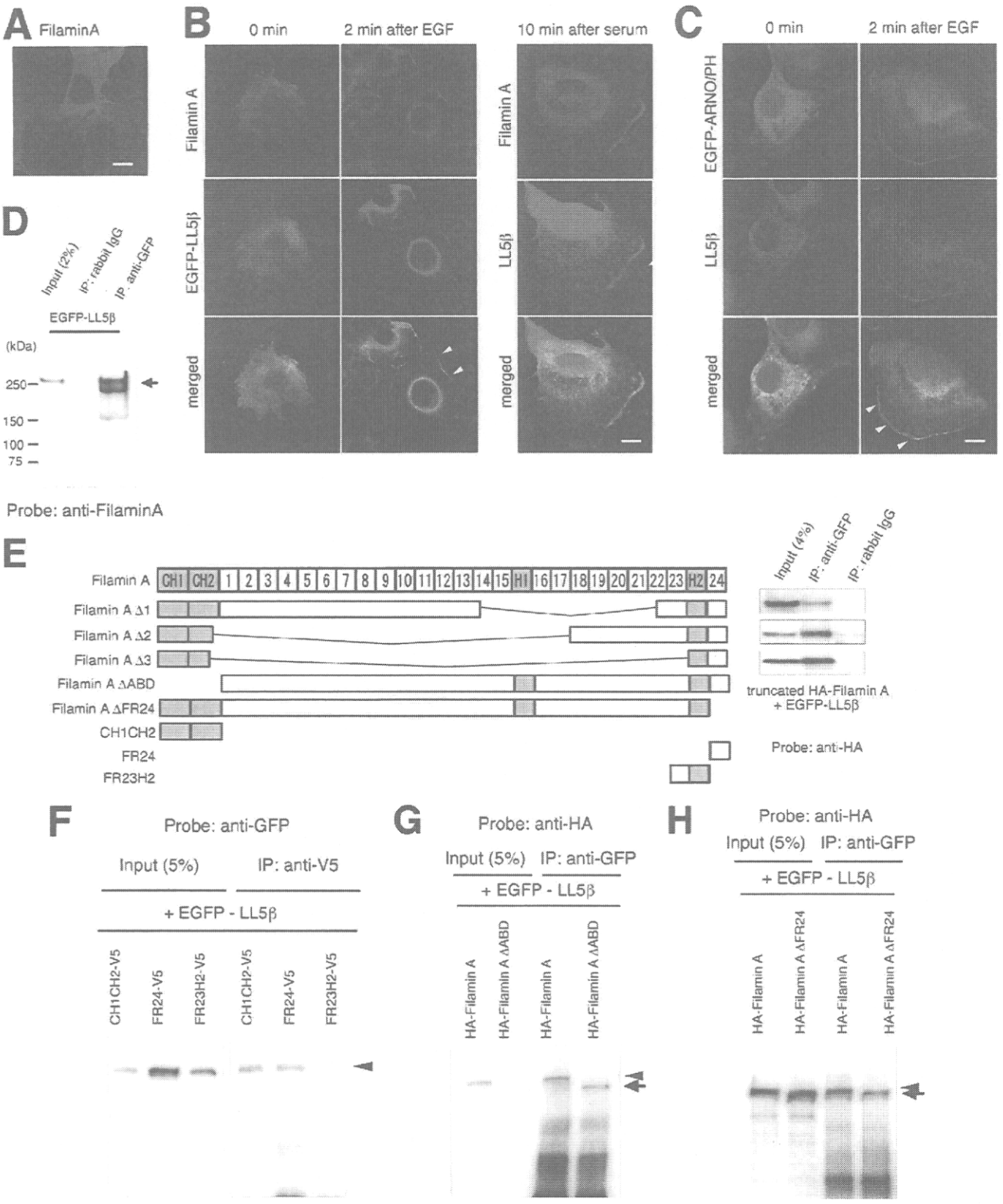

and a PH domain that is highly specific for PtdIns(3,4,5)P_3 (10, 11). It has been reported that LL5β binds to exogenous Filamin A, as well as Filamin C (12), *in vitro*. However, the LL5β and Filamin A regions required for binding and the biological significance of LL5β-Filamin A binding have not been experimentally explored.

It has been shown that SHIP2 is a critical component of a negative feedback loop that regulates PtdIns(3,4,5)P_3 levels in nerve growth factor-stimulated PC12 cells, together with the constitutively active phosphatidyl inositol-3 (PtdIns-3) phosphatase, phosphatase and tensin homologue deleted on chromosome 10 (PTEN) (13). This suggests that SHIP2 contributes to establishing a narrow accumulation of PtdIns(3,4,5)P_3 in the membrane. Because PtdIns(3,4,5)P_3 works as an internal compass of polarity in directed migrating cells, SHIP2 is likely to help a cell respond accurately and dynamically to external signals that impart directionality by increasing PtdIns(3,4,5)P_3 levels in a leading edge of the cell. Previous studies have demonstrated that SHIP2 binds to Filamin A and that Filamin A is essential for the translocation of SHIP2 to the membrane ruffle. Moreover, recombinant SHIP2 regulates PtdIns(3,4,5)P_3 levels and the distribution of submembranous actin at membrane ruffles following growth factor stimulation (14). However, it remains elusive as to how and what molecules control SHIP2 and Filamin A translocation to the membrane, where in the cell periphery SHIP2 translocates, how membranous PtdIns(3,4,5)P_3 levels are regulated by translocation of SHIP2, and how submembranous actins are controlled.

EXPERIMENTAL PROCEDURES

Details of experimental procedures are provided in the supplemental Experimental Procedures.

Isolation of LL5β cDNA—The full-length human LL5β cDNA (GenBank™ accession number AJ496194) was cloned from a human placenta cDNA library (BD Biosciences).

Plasmid Vectors—Full-length LL5β cDNA was subcloned into pEGFP-C3 (plasmid vector for expressing enhanced green fluorescent protein-C3, Clontech) to generate pEGFP-LL5β. In addition, expression vectors for human LL5β lacking the first 156 amino acid residues (pEGFP-LL5βΔN1, we designated this vector as ΔN1), 323 amino acid residues (pEGFP-LL5βΔN2 as ΔN2), and 488 amino acid residues (pEGFP-LL5βΔN3 as ΔN3) were generated using pEGFP-C3. pEGFP-C3 was also used for enhanced green fluorescent protein (EGFP) expression in COS-7 cells. Procedures for generating ΔN4, ΔN5, Δ2-a to Δ2-e, LL5βΔPH, and LL5β-VSV are described in the supplemental Experimental Procedures. Other protein expression vectors were constructed using pCAGGS so that the cDNAs would be driven under a modified chicken β-actin (CAG) promoter. We used pCAGGS-hemagglutinin (HA)-tagged Filamin A (pCAGGS-HA-Filamin A) (15). The following vectors were also generated: pCAGGS-HA-Filamin A truncated mutant 1 (Filamin AΔ1), pCAGGS-HA-Filamin A truncated mutant 2 (Filamin AΔ2), pCAGGS-HA-Filamin A truncated mutant 3 (Filamin AΔ3), and pCAGGS-HA-Filamin without repeat 24 (Filamin A ΔFR24). In addition, various vectors that expressed Val-Val-Val-Val-Val (V5)-His-tagged Filamin A fragments were constructed: CH1CH2, which contains the actin-binding domain 1 (CH1) and domain 2 (CH2) of Filamin A; FR24, which contains the filamin repeat (FR, also called immunoglobulin-like-β-sheet motif) 24 of Filamin A; and FR23H2, which contains the filamin repeat 23 and hinge 2 (H2) of Filamin A. The generation of Filamin AΔABD (ABD, actin-binding domain) has been described previously (15). For Filamin C expression, we used pBudCE4-Filamin C (made using pZP7-Filamin C, a generous gift from Dr. D. W. Chung, and pBudCE4 from Invitrogen). Full-length rat SHIP2 (GenBank accession number NM_022944) cDNA was subcloned into pCAGGS-GFP or pmCherry-N1 (Clontech) to generate SHIP2-expressing vector, where mCherry is a mutant fluorescent protein derived from the tetrameric *Discosoma* sp. red fluorescent protein (DsRed). The PH domain of rat ADP-ribosylation factor (ARF) nucleotide-binding size opener (16, 17) (ARNO, GenBank accession number NM_053911, gift from Dr. T. Balla) was subcloned into pCAGGS-GFP vector to generate EGFP-ARNO/PH-expressing vector. The PH domain of mouse general receptor for phosphoinositides 1 (18) (GRP1, GenBank accession number BC035296.1) was subcloned into pEGFP-C1 to generate EGFP-GRP1/PH-expressing vector.

Antibodies—The following antibodies were used: anti-GFP antibody that can recognize EGFP (MBL Medical and Biological Laboratories, Nagoya, Japan), anti-Filamin A antibody (MAB1678, Chemicon), anti-HA antibody (sc-805, Santa Cruz Biotechnology, Santa Cruz), anti-α-tubulin (DM1A, Sigma), anti-VSV antibody (P5D4, Sigma), anti-pan-cadherin antibody (CH-19, Sigma), anti-glyceraldehyde-3-phosphate dehydrogenase antibody (14C10, Cell Signaling Technology, Danvers, MA), anti-rabbit IgG (Sc-2027, Santa Cruz Biotechnology), anti-V5 antibody (Invitrogen), anti-β actin antibody (AC-40, Sigma), anti-FLAG antibody (F3165, Sigma), anti-PtdIns(3,4,5)P_3 antibody (F3165, NN111.1.1, MBL Medical and Biological Laboratories), Alexa

FIGURE 1. **LL5β binds to Filamin A through its CH1CH2 or repeat 24.** *A*, distribution of Filamin A in COS-7 cells without exogenous LL5β. *Scale bar* = 10 μm. *B*, *left* and *middle columns*, following EGF application, exogenous EGFP-LL5β (*green*) and endogenous Filamin A (*red*) colocalized at the plasma membrane (*arrowheads*). *Right column*, endogenous Filamin A (*red*) and endogenous LL5β (*green*) were visualized in COS-7 cells that had been cultured without serum for 18 h. They accumulated near the plasma membrane at 10 min after the addition of 10% serum. *Scale bar* = 10 μm. *C*, following EGF application, exogenous EGFP-tagged ARNO/PH (EGFP-ARNO/PH) (*green*) and endogenous LL5β (*red*) colocalized at the plasma membrane (*arrowheads*). *Scale bar* = 10 μm. *D*, lysates from COS-7 cells expressing EGFP-LL5β were subjected to immunoprecipitation (*IP*) with an anti-GFP antibody or rabbit IgG (control). Endogenous Filamin A (~280 kDa, *arrow*) was co-immunoprecipitated with EGFP-LL5β. *E*, schematic drawings show the various truncated Filamin A mutants. They were tagged with HA at their amino termini. EGFP-LL5β was co-expressed in COS-7 cells with one of the truncated Filamin A mutants, as shown on the *left*, followed by immunoprecipitation with anti-GFP antibody or rabbit IgG (control) and detection with anti-HA antibody. Filamin A mutants (Filamin AΔ1-Δ3) were co-immunoprecipitated. *CH1* and *CH2*, actin-binding site 1 and 2, respectively. *H1* and *H2*, hinge 1 and 2. *Numbers* (1–24) indicate the FR number. *F*, CH1CH2, FR24, or FR23H2 (Filamin repeat 23 and hinge 2) tagged with V5 were co-expressed with EGFP-LL5β. EGFP-LL5β was co-immunoprecipitated with CH1CH2 or FR24 but not FR23H2 (*arrowhead*). *G*, full-length Filamin A (*arrowhead*) or Filamin AΔABD (*arrow*) tagged with HA was co-immunoprecipitated with EGFP-LL5 β. *H*, full-length Filamin A (*arrowhead*) or Filamin A ΔFR24 (*arrow*) tagged with HA was co-immunoprecipitated with EGFP-LL5β.

LL5β-Filamin A-SHIP2 Leads to Steeper PtdIns(3,4,5)P_3 Accumulation

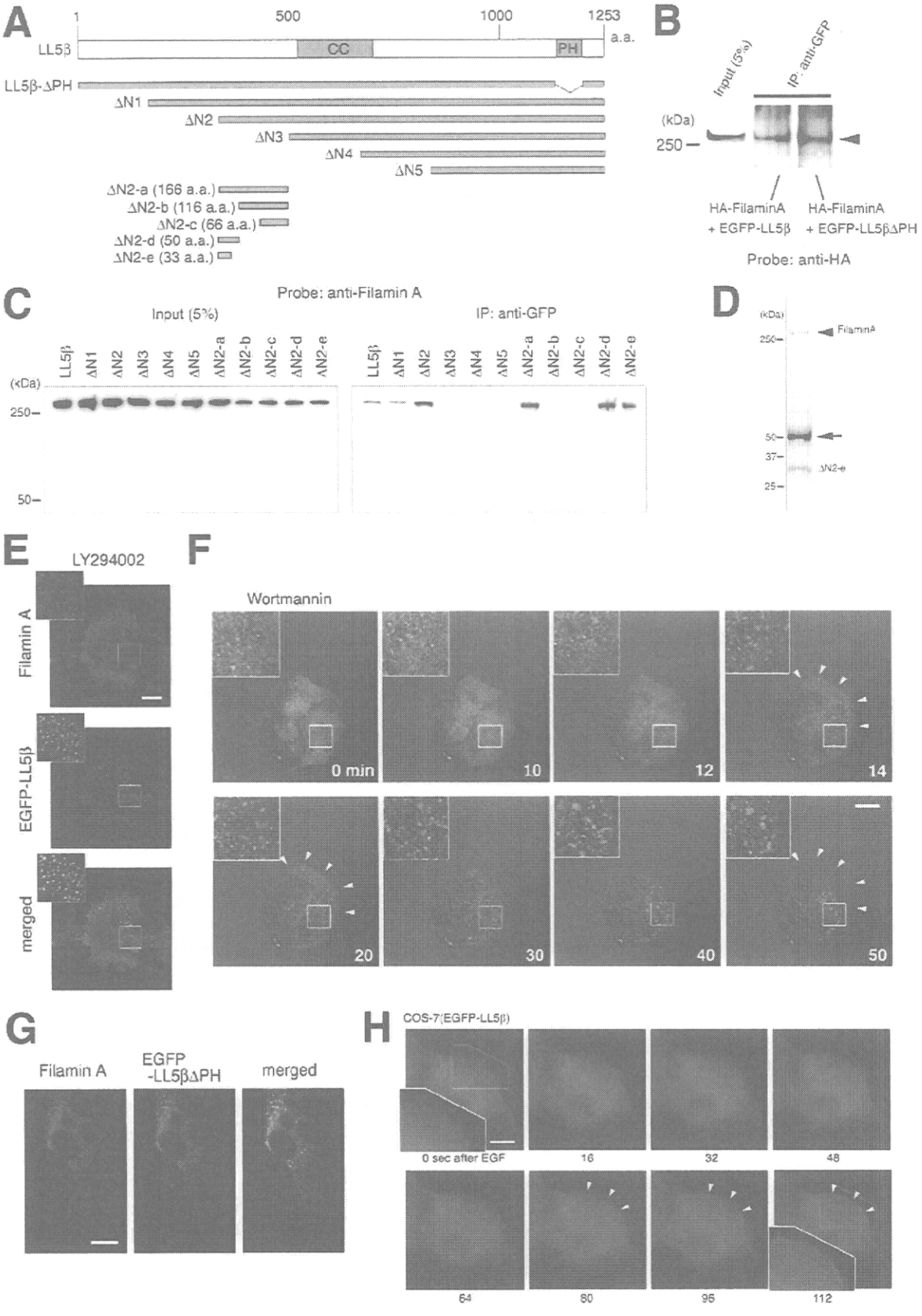

Fluor 568 phalloidin (Invitrogen). Anti-LL5β polyclonal antibody was generated in cooperation with SIGMA Genosys Japan (Ishikari, Japan).

Cell Culture and DNA Transfection—COS-7 cells were used. Vectors were transfected using PolyFect transfection reagent (Qiagen, Hilden, Germany) or FuGENE 6 transfection reagent (Roche Diagnostics). To increase PtdIns (3,4,5)P_3 in the plasma membrane, cells were cultured without serum for 16–18 h and then cultured with epidermal growth factor (EGF) for 2 min or serum for 10 min. Human melanoma cell lines M2 and A7 were maintained as reported previously (4). FuGENE HD (Roche Diagnostics) was used to transfect these cells.

F-actin Staining, Immunocytochemistry, Analyses of Cell Motility, and Reverse Transcription-PCR—Conventional protocols were used.

Immunoprecipitation, Western Blotting (Immunoblotting) Analyses, and MALDI-TOF Mass Spectrometry—Immunoprecipitation was performed with Dynabeads (Dynal, Hamburg, Germany) coated with antibodies specific to rabbit or mouse IgG. Matrix-assisted laser desorption ionization/time of flight (MALDI-TOF) mass spectrometry (Bruker Daltonics, Billerica, MA) was used for protein identification.

RNA Interference—Three different constructs of LL5β short hairpin RNA (shRNA) were prepared in the mouse U6 snRNA promoter (mU6pro) vector (mU6pro-LL5β-RNAi), which has a mouse U6 promoter (15). Their sequence targets were nucleotides 177–197, 2246–2266, and 3647–3667 of the human LL5β cDNA. These shRNAs were termed LL5β-shRNA1, LL5β-shRNA2, and LL5β-shRNA3 and such vectors were called LL5β-RNAi1, LL5β-RNAi2, and LL5β-RNAi3, respectively. For co-transfection, a molar ratio of 1 (EGFP expression plasmid) to 2 (LL5β-RNAi or empty mU6pro vector) was employed. Empty shRNA vector was used as a control.

Wound-healing Assay—Overconfluent COS-7 cells were co-transfected with pEGFP-C3 and mU6pro-LL5β-RNAi vector or pEGFP-C3 and control vector. Empty shRNA vector was used as the control vector. After 36–48 h, the confluent cell layer was disrupted followed by a 3-h incubation. After fixing and staining with rhodamine-phalloidin, cells at the defect edge expressing EGFP were observed, and the numbers of cells with or without lamellipodia were counted.

PI3K Inhibition and Time-lapse Observation—For PI3K inhibition experiments, cells were cultured for 18–24 h followed by the addition of wortmannin (Sigma, final concentration 100 nM) or LY294002 (Sigma, final concentration 10 μM). Time-lapse observation was started (time 0) in a CO_2 incubation chamber (5% CO_2 at 37 °C) fitted onto a confocal microscope. Images were obtained every 1–2 min for 15 min to 1 h. Confocal images or live cell images were captured. Images were obtained using an AxioCam (Carl Zeiss, Oberkochen, Germany).

Subcellular Fractionation—Subcellular fractionation was performed using the ProteoExtract subcellular proteome extraction kit (Calbiochem) in accordance with the manufacturer's instructions. Utilizing the different extraction buffers in the kit, four different fractions were separated. The Triton-insoluble membrane/organelle fractions are shown in Fig. 5*E*. The amounts of the pan-cadherin (as reference for membrane proteins) and glyceraldehyde-3-phosphate dehydrogenase were used as internal controls.

Statistical Analyses—Significant differences, as indicated by $p < 0.01$, were determined by the non-parametric Mann-Whitney *U* test or *t* test.

RESULTS

First of all, we experimentally examined the relationship between LL5β and Filamin A (Fig. 1*A*) and their regions responsible for interaction. We expressed LL5β, tagged with EGFP at its amino terminus (EGFP-LL5β), in COS-7 cells to determine whether LL5β colocalizes with endogenous Filamin A (Fig. 1*B*). EGFP-LL5β and endogenous Filamin A colocalized primarily at the cell periphery after EGF application (final concentration, 100 ng/ml; Fig. 1*B*, *left* and *middle columns*), as reported previously (11). Endogenous LL5β (supplemental Fig. S1) colocalized with endogenous Filamin A at the cell periphery by serum stimulation (Fig. 1*B*, *right column*). Previous work has demonstrated that PI3K is activated by EGF (17) or by serum stimulation (19). EGFP-tagged ARNO-PH, which specifically binds to PtdIns(3,4,5)P_3, has been used as a PtdIns(3,4,5)P_3 detector (16, 17). Two minutes after EGF application, ARNO-PH accumulated at the cell periphery together with endogenous LL5β (Fig. 1*C*), suggesting that LL5β translocates where PtdIns(3,4,5)P_3 localizes. EGF-induced accumulation of PtdIns(3,4,5)P_3 at the cell periphery was further confirmed by another PtdIns(3,4,5)P_3 detector GRP1/PH (18) or immunocytochemical techniques (supplemental Fig. S2).

The interaction between LL5β and Filamin A was confirmed by immunoprecipitation. Cell lysates from COS-7 cells expressing EGFP-LL5β, an anti-GFP antibody that is capable of recognizing EGFP, and an anti-Filamin A antibody were used. This anti-Filamin A antibody did not cross-react with Filamin C in lysates from Filamin C-overexpressing COS-7 cells (data not shown). Filamin A, which is ~280 kDa (3, 20), was co-immu-

FIGURE 2. **The LL5β-Filamin A complex changes its subcellular localization depending on the level of membrane phosphatidylinositol 3,4,5-triphosphate.** *A*, schematic drawings show full-length and various truncated mutants of LL5β. *a.a.*, amino acids, *CC*, putative coiled-coil region. *B*, HA-Filamin A was co-immunoprecipitated with EGFP-LL5βΔPH as well as EGFP-LL5β (*arrowhead*). *C*, endogenous Filamin A was co-immunoprecipitated (*IP*) in with LL5β or LL5β mutants ΔN1, ΔN2, ΔN2-a, ΔN2-d, or ΔN2-e. *D*, ΔN2-e tagged with EGFP was expressed in COS-7 cells and then immunoprecipitated with anti-GFP antibody. Immunoprecipitates were subjected to SDS-PAGE. Filamin A detected by MALDI-TOF mass spectrometry is noted (*arrowhead*). The *arrow* indicates the IgG heavy chain band. *E*, the PI3K inhibitor LY294002 was applied to COS-7 cells expressing EGFP-LL5β. Exogenous EGFP-LL5β (*green*) as well as endogenous Filamin A (*red*) exhibited a punctate distribution with little expression at the cell periphery. The two proteins colocalized well. Each *inset* shows higher magnification views of the area indicated by the *square* in the same panel. *Scale bar* = 10 μm. *F*, temporal profiles of subcellular localization of EGFP-LL5β (*green*). The PI3K inhibitor wortmannin (100 nM) was applied to COS-7 cells at time 0. Each *inset* shows higher magnification views of the area indicated by the *square* in the same panel. Translocation of EGFP-LL5β to the cytosol as well as puncta formation began in about 14 min. The cell edge is indicated by *arrowheads*. *Scale bar* = 10 μm. *G*, EGFP-LL5βΔPH (*green*) showed a punctate distribution in COS-7 cells, colocalizing well with endogenous Filamin A (*red*), which also exhibited a punctate distribution. *Scale bar* = 10 μm. *H*, EGFP-LL5β (*green*) accumulated in the membrane in 80 s following the application of EGF (final concentration of 100 ng/ml) in COS-7 cells that had been serum-starved for 18 h. Each *inset* shows higher magnification views of the area indicated by the *pentagon* in the same panel. *Arrowheads* indicate the recruitment of EGFP-LL5β near the plasma membrane. *Scale bar* = 10 μm.

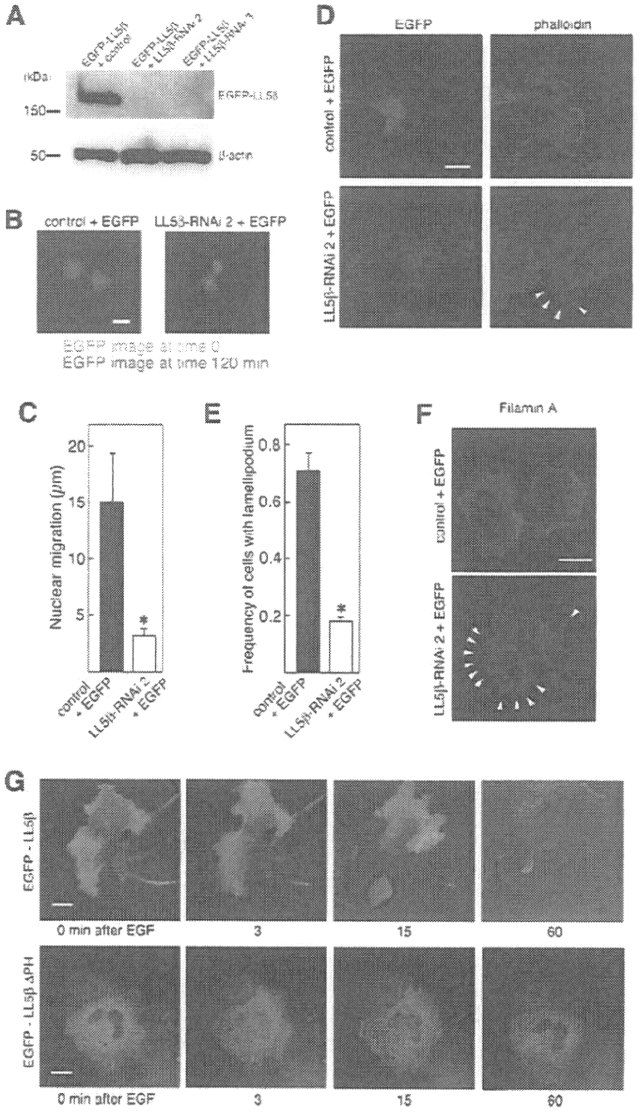

FIGURE 3. **Knockdown of LL5β decreases cell motility and lamellipodium formation.** *A*, LL5β-RNAi2 or LL5β-RNAi3 were co-transfected with the EGFP-LL5β expression vector in COS-7 cells. The knockdown efficiency of each RNAi was evaluated by estimating the EGFP signal intensity. *B*, EGFP expression vector and empty mU6pro vector (control) (*left*) or EGFP expression vector and LL5β-RNAi vector (LL5β-RNAi 2) (*right*) were transfected into COS-7 cells that had been cultured under low cell density conditions. EGFP images (*green*) were acquired at an interval of 120 min and merged together after the color of the later images had been converted to red. Knockdown of LL5β resulted in a decrease in cell motility. *Scale bar* = 50 μm. *C*, to quantify cell motility, the migrated distance (mean ± S.E.) of each nucleus during the 120-min interval was measured for each group (n = 50 each). * indicates statistical significance ($p < 0.01$). *D*, the EGFP expression vector was transfected into COS-7 cells together with an empty mU6pro vector (control) (*upper panels*) or LL5β-RNAi vector (*lower panels*). EGFP-positive (transfected) cells were studied. F-actin localization was visualized simultaneously with rhodamine-phalloidin or Alexa Fluor 568 phalloidin. Knockdown of LL5β resulted in the frequent formation of small protrusions (*arrowheads*) and in a decrease in lamellipodium formation. *Scale bar* = 10 μm. *E*, the number of cells with lamellipodia (with an edge line equal to or longer than 10 μm) in *panel D* was counted among randomly selected EGFP-positive cells (mean ± S.E.). n = 90 for both cases (three independent experiments, n = 30 each). *, $p < 0.01$. *F*, the peripheral distribution of endogenous Filamin A was impaired by knocking down LL5β. Only fiber-like Filamin A was observed in small protrusions (*arrowheads*). The EGFP expression vector was co-transfected, and EGFP-positive cells were studied (EGFP images were not shown). *Scale bar* = 10 μm. *G*, culture medium containing 100 ng/ml EGF was added (0 min) to COS-7 cells expressing EGFP-LL5β or EGFP-LL5βΔPH after being cultured without serum for 18 h. EGFP-LL5β-expressing cells responded strongly and dramatically changed their morphology, whereas those with EGFP-LL5βΔPH did not. *Scale bar* = 20 μm.

noprecipitated with EGFP-LL5β (Fig. 1*D*). We then searched for the region of Filamin A responsible for this interaction. Filamin A, which usually exists as a homodimer, contains an amino-terminal actin-binding domain that precedes 24 immunoglobulin-like β-sheet motifs (FR, filamin repeats) (Fig. 1*E*). The last FR (FR 24) is responsible for homodimerization (20). Using three deletion mutants of amino-terminally HA-tagged Filamin A that lack different regions of the immunoglobulin-like-β-sheet motifs (Filamin AΔ1-Filamin AΔ3), we identified the domain of Filamin A responsible for its interaction with LL5β (Fig. 1*E*). Even Filamin AΔ3, which includes hinge 1 but lacks FR1–23, was co-immunoprecipitated with EGFP-LL5β (Fig. 1*E*). We next assessed the ability of the two actin-binding motifs (CH1, CH2), FR24 and hinge 2 (H2) of Filamin A, to bind to EGFP-LL5β. Two Filamin A fragments, CH1CH2 and FR24, but not FR23H2, were co-immunoprecipitated with EGFP-LL5β (Fig. 1, *E* and *F*). Furthermore, HA-tagged Filamin A without actin-binding domain (HA-Filamin A ΔABD) or without FR24 (HA-Filamin A ΔFR24) was co-immunoprecipitated with EGFP-LL5β (Fig. 1, *E*, *G*, and *H*). These results suggest that both the actin-binding domain and the FR24 of Filamin A are responsible for an interaction with LL5β.

We next determined which domains of LL5β are required for this interaction (Fig. 2*A*). First, we generated a mutant of LL5β that lacks the PH domain (LL5βΔPH). HA-tagged Filamin A was co-expressed with EGFP-tagged LL5β (EGFP-LL5β) or EGFP-tagged LL5βΔPH (EGFP-LL5βΔPH) in COS-7 cells followed by lysis and immunoprecipitation with an anti-GFP antibody. Co-immunoprecipitated HA-tagged Filamin A was observed with the similar intensity in lysates from cells co-expressing either EGFP-LL5β or EGFP-LL5βΔPH (Fig. 2*B*), indicating that the PH domain is not required for binding to Filamin A. We then used various truncated forms of LL5β with N-terminal EGFP tags to search for regions of LL5β responsible for Filamin A binding. A Filamin A interaction occurred with ΔN1 and ΔN2, but not with the ΔN3, ΔN4, or ΔN5 mutants of LL5β, indicating that a domain present in ΔN2 but not ΔN3 is responsible for this interaction. We then further truncated this domain and found that ΔN2-a, but not ΔN2-b or ΔN2-c, could interact. Finally, we discovered that a 33-amino acid region (323–356, ΔN2-e) was sufficient for binding (Fig. 2*C*). This binding region of LL5β was different from what has been previously documented (12). To confirm our observation, we expressed ΔN2-e in COS-7 cells and identified co-immunoprecipitated proteins using MALDI-TOF mass spectrometry. Then, Filamin A was identified (Fig. 2*D*). We reconfirmed our results.

Because the PH domain of LL5β is specifically sensitive to PtdIns(3,4,5)P_3 (10), we next examined whether the recruitment of LL5β to the lamellipodia is driven by PtdIns(3,4,5)P_3. Because the phosphorylation state of PtdIns(3,4,5)P_3 is regulated by the phosphorylation of phosphatidylinositol 4,5-biphosphate by PI3K, COS-7 cells with exogenous EGFP-LL5β were treated with the PI3K inhibitor, LY294002. After this

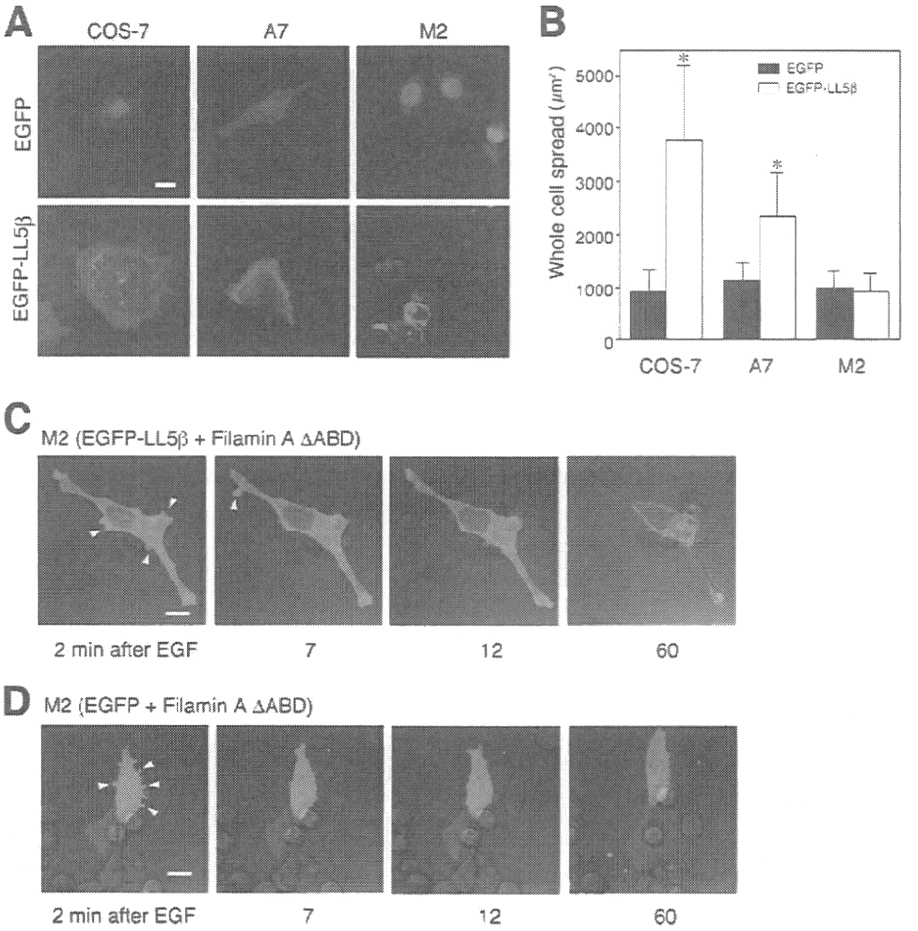

FIGURE 4. **Filamin A is necessary for induction of lamellipodium formation by LL5β.** *A*, EGFP expression vector or EGFP-LL5β expression vector was transfected into COS-7 cells, A7 cells (which contain Filamin A), and M2 cells (which lack Filamin A). Very large lamellipodia were developed in the presence of EGFP-LL5β in COS-7 cells and A7 cells but not in the M2 cells. *Scale bar* = 10 μm. *B*, a whole-cell area was measured from 50 cells; cells were randomly selected in each case (mean ± S.E.). * $p < 0.01$. *C* and *D*, M2 cells expressing EGFP-LL5β and Filamin AΔABD or EGFP and Filamin AΔABD were cultured without serum for 18 h. EGF (final concentration 100 ng/ml) was then added into the culture medium (time 0). Approximately 2 min after EGF addition, small pseudopods (*arrowheads*) were transiently generated. The images were merged with their differential interference contrast images. *Scale bars* = 10 μm.

treatment, EGFP fluorescence was distributed in a punctate manner and colocalized with endogenous Filamin A (Fig. 2*E*; supplemental Fig. S3; supplemental Video 1). No accumulation of Filamin A was observed at the cell periphery. Our time-lapse study gave us more detailed information on how this redistribution took place. Puncta were formed in COS-7 cells about 14 min after treatment with the PI3K inhibitor, wortmannin (Fig. 2*F*). The EGFP-LL5β signal was not observed in lamellipodia after this treatment (Fig. 2*F*). This observation was further investigated by overexpressing EGFP-LL5βΔPH. EGFP-LL5βΔPH did not localize to the plasma membrane but colocalized well with endogenous Filamin A in a punctate distribution in the cytoplasm (Fig. 2*G*). This result is consistent with the demonstration of LL5βΔPH binding to HA-tagged Filamin A (Fig. 2*B*). We further examined the spatiotemporal regulation of LL5β in response to PtdIns(3,4,5)P_3. We added EGF to the culture medium after serum depletion for 16–18 h and continuously observed changes in EGFP-LL5β localization. Recruitment of EGFP-LL5β to the plasma membrane was first observed ~80 s after EGF application, and by 112 s, EGFP-LL5β accumulated along the plasma membrane (Fig. 2*H*; supplemental Video 2). These data suggest that LL5β changes its subcellular localization quickly enough to chase changeable PtdIns(3,4,5)P_3 distribution (supplemental Fig. S4 and supplemental Video 3).

The ability of LL5β to bind to Filamin A, a protein crucial for cell motility (20), suggests that LL5β is also involved in motility control. To investigate the function of LL5β, we carried out LL5β knockdown experiments using RNA interference (RNAi). Of the three different shRNA constructs against LL5β, we found that LL5β-RNAi2 and LL5β-RNAi3 suppressed the expression of EGFP-LL5β with similar efficiency (Fig. 3*A*; supplemental Fig. S5). In the following experiments, we primarily used LL5β-RNAi2 to suppress LL5β expression in COS-7 cells, but LL5β-RNAi3 gave us similar results (supplemental Fig. S6). LL5β-RNAi reduced cell motility when compared with control cells under low cell density conditions where cells could move freely (Fig. 3, *B* and *C*). We then employed a wound-healing assay to determine whether there was any alteration to the cell-crawling machinery (Fig. 3, *D* and *E*). In this assay, quiescent cells in an overconfluent state usually develop lamellipodia in response to the removal of neighboring cells. We found that "typical lamellipodia" (defined as edge lines equal to or more than 10 μm long) were not properly formed in cells with LL5β-RNAi. Instead, small protrusions that contained F-actin (with edge lines less than 10 μm long) were observed (Fig. 3*D*). The frequency of cells with lamellipodia was estimated with or without LL5β-RNAi. Knockdown of LL5β resulted in a decrease in lamellipodium formation (Fig. 3*E*), suggesting that LL5β is essential for lamellipodium formation in COS-7 cells. Moreover, when LL5β expression was down-regulated by the RNAi technique in COS-7 cells, the distribution of Filamin A near the plasma membrane was significantly altered (Fig. 3*F*). Reduced formation of lamellipodia and a fiber-like distribution of Filamin A were observed in the small protrusions seen in LL5β knockdown cells. In contrast, LL5β overexpression resulted in the formation of large lamellipodia (Figs. 3*G*, *upper row*, and 4*A*, *left* and *middle panels*). In response to EGF, COS-7 cells with exogenous LL5β became very active (supplemental Video 4), whereas those with exogenous LL5βΔPH did not (Fig. 3*G*, *lower row*), indicating that the

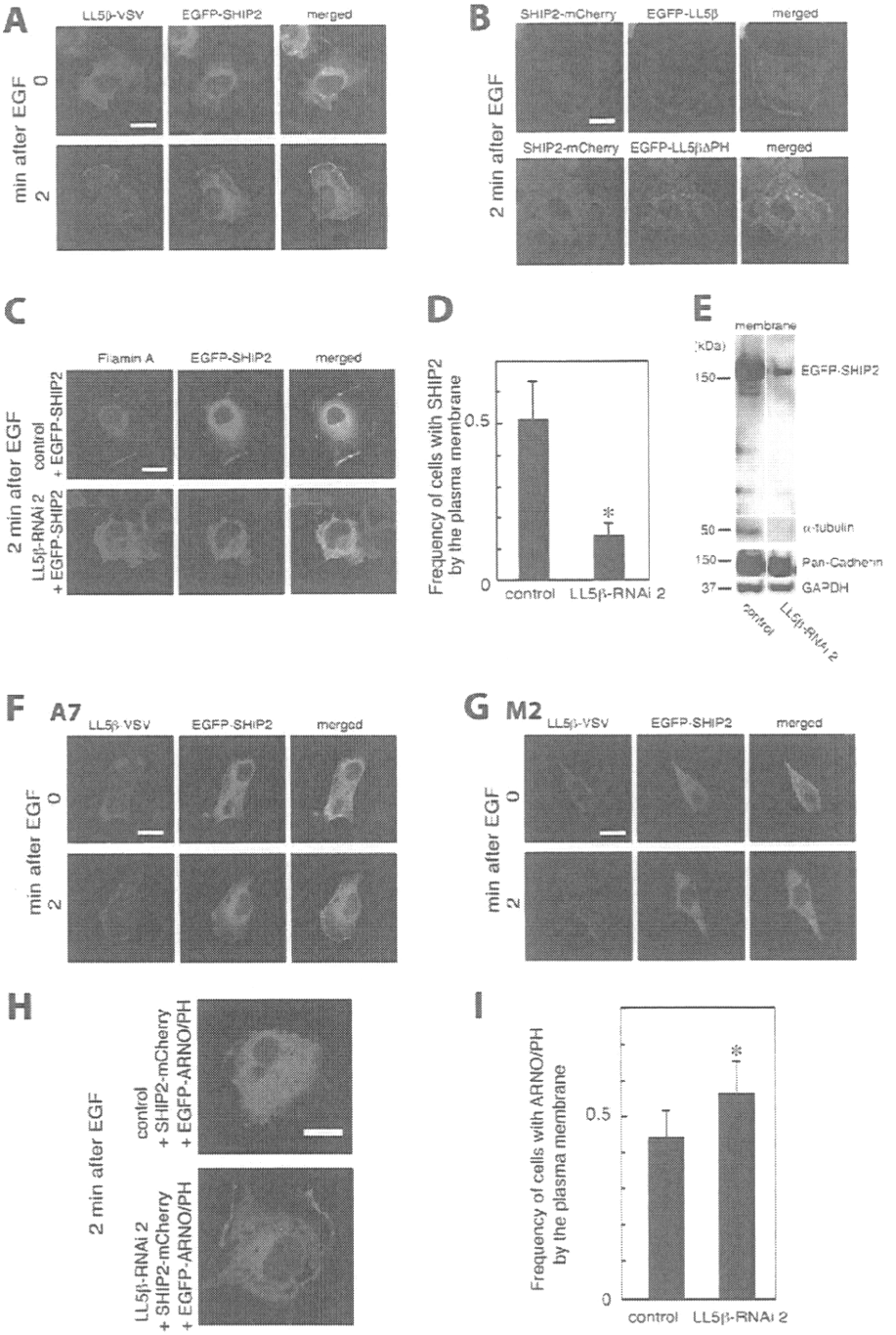

FIGURE 5. **LL5β directs membrane localization of SHIP2, and PtdIns(3,4,5)P$_3$ localization is mutually modified by co-recruited SHIP2.** In the following cases, cells were serum-starved for 16–18 h and then stimulated with the final concentration of 100 ng/ml EGF for 2 min. *A*, LL5β tagged with VSV (LL5β-VSV) was co-expressed with EGFP-SHIP2 in COS-7 cells. VSV signals (*red*) accumulated near the plasma membrane 2 min after EGF stimulation. *Scale bar* = 10 μm. *B*, SHIP2 tagged with mCherry (SHIP2-mCherry) and EGFP-LL5β or EGFP-LL5βΔPH were co-transfected into COS-7 cells. SHIP2-mCherry (*red*) and EGFP-LL5β (*green*) accumulated near the plasma membrane (*upper row*), whereas SHIP2-mCherry and EGFP-LL5βΔPH (*green*) did not (*lower row*). *Scale bar* = 10 μm. *C*, knockdown of LL5β resulted in a decrease in the membrane localization of SHIP2 (*lower row*). Empty mU6pro vectors were used for control. *Scale bar* = 10 μm. *D*, the frequency of cells with membrane-localized SHIP2 in *panel C* was determined among randomly selected EGFP-positive cells (mean ± S.E., three independent experiments, $n = 50$ cells each). *, $p < 0.01$. *E*, knockdown of LL5β resulted in reduced membrane translocation of EGFP-SHIP2. COS-7 cells in *panel C* were subjected to subcellular fractionation. The amount of SHIP2 in the membrane fractions was analyzed by immunoblotting with anti-GFP antibody. Unexpectedly, α-tubulin was decreased in LL5β knockdown cells. The amounts of cadherins (detected by pan-cadherin antibody) and glyceraldehyde-3-phosphate dehydrogenase (*GAPDH*) were used as a reference. *F* and *G*, LL5β-VSV and EGFP-SHIP2 expression vector were transfected into A7 cells and M2 cells. LL5β-VSV (*red*) and EGFP-SHIP2 (*green*) accumulated near the plasma membrane in A7 cells (*F*), but not in M2 cells (*G*), by the addition of EGF. *Scale bar* = 10 μm. *H*, EGFP-ARNO/PH, SHIP2-mCherry, and control (empty mU6pro vector) or LL5β-RNAi2 were co-transfected into COS-7 cells. Knockdown of LL5β resulted in an increase in membrane-localized EGFP-ARNO/PH (*green*). *Scale bar* = 10 μm. *I*, the frequency of cells with membrane-localized EGFP-ARNO/PH in *panel H* was determined among randomly selected EGFP-positive cells (mean ± S.E., three independent experiments, $n = 50$ cells each). *, $p < 0.01$.

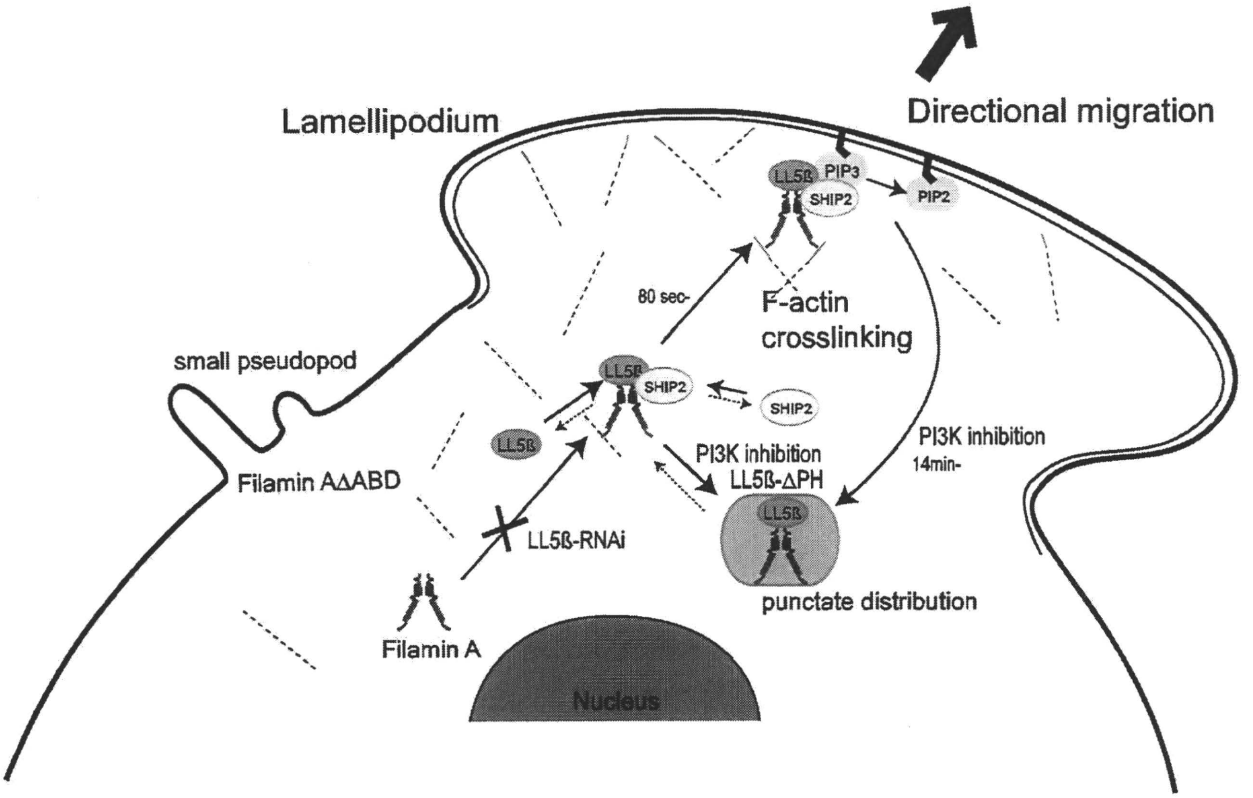

FIGURE 6. **Role of the LL5β-Filamin A-SHIP2 complex during PtdIns(3,4,5)P_3-mediated directed migration.** In directed migrating cells, PtdIns(3,4,5)P_3 accumulates in their leading edge. LL5β controls the spatial distribution and activity of Filamin A depending on the localization of membranous PtdIns(3,4,5)P_3 (shown as *PIP_3*). LL5β enhances lamellipodium formation by possibly increasing the cross-linking of newly polymerized F-actin at the plasma membrane (shown in *red*) by recruiting the F-actin-cross-linking molecule, Filamin A, to the plasma membrane. SHIP2 is co-recruited to sites of PtdIns(3,4,5)P_3 accumulation by LL5β via Filamin A, and then it reciprocally dephosphorylates PtdIns(3,4,5)P_3 to phosphatidylinositol 3,4-biphosphate (PtdIns(3,4)P_2, shown as *PIP_2*).

PH domain of LL5β is critical for this action. Because the PH domain of LL5β is primarily sensitive to PtdIns(3,4,5)P_3(10, 11) and because PtdIns(3,4,5)P_3 is generated at the plasma membrane upon EGF application (17), it is probable that the binding of LL5β to membrane PtdIns(3,4,5)P_3 induced this cellular response.

Because LL5β overexpression in COS-7 cells resulted in the enlargement of the peripheral area (including lamellipodia) of cells, we next examined whether Filamin A is involved in this response. M2 cells, in which LL5β mRNA was not detected (data not shown), are derived from a human melanoma and do not express Filamin A, whereas A7 cells are generated by stably transfecting Filamin A cDNA into M2 cells (4). These cells express a molar ratio of Filamin A to actin comparable with that found in cells normally expressing Filamin A (4). The LL5β-induced enlargement was observed in A7 cells as well as COS-7 cells, but not in M2 cells (Fig. 4, *A* and *B*), suggesting that enlargement induced by LL5β overexpression requires Filamin A. The versatility of Filamin A led us to ask whether the F-actin-cross-linking activity of Filamin A is essential for this enlargement. Filamin A dimerized through their carboxyl termini, and then dimerized Filamin A cross-linked two F-actin molecules through their ABD at their amino termini (15, 21). Thus, we transfected a Filamin AΔABD expression vector (15) into M2 cells and examined the Filamin A F-actin-cross-linking activity to that observed in A7 cells. Application of EGF resulted in the formation of small pseudopods, but not proper lamellipodia, in M2 cells transfected with EGFP-LL5β and Filamin AΔABD (Fig. 4*C*). Therefore, the actin binding activity, or probably the F-actin-cross-linking activity, of Filamin A is crucial for the LL5β-mediated formation of lamellipodia. Because EGF induced small pseudopods in M2 cells transfected with Filamin AΔABD even in the absence of LL5β (Fig. 4*D*), it is unlikely that LL5β is involved in the formation of these small pseudopods.

We next sought to determine whether LL5β directs translocation of SHIP2-Filamin A complex. As reported (14), SHIP2 interacts with Filamin A (data not shown). By contrast, direct interaction between SHIP2 and LL5β was not observed (supplemental Fig. S7), suggesting that LL5β directs subcellular localization of SHIP2 via Filamin A. Two minutes after EGF stimulation, EGFP-tagged SHIP2 (EGFP-SHIP2) or mCherry-tagged SHIP2 (SHIP2-mCherry) localized to the cell periphery with LL5β (Fig. 5, *A*, *lower row*, and *B*, *upper row*) but remained in the cytosol in the presence of LL5βΔPH (Fig. 5*B*, *lower row*). As expected, SHIP2 colocalized well with Filamin A (Fig. 5*C*, *upper row*), but translocation of SHIP2 to the cell membrane was observed less in LL5β knockdown COS-7 cells (Fig. 5, *C*, *lower row*, and *D*). Supporting this observation, the amount of SHIP2 in the membrane fraction was reduced in LL5β knockdown COS-7 cells (Fig. 5*E*). These data indicate that Filamin A is an intermediate between LL5β and SHIP2. Indeed, translo-

cation of EGFP-SHIP2 and LL5β to the cell periphery was observed in A7 cells (Fig. 5*I*). In M2 cells (Filamin A-deficient A7 cells), LL5β was translocated to the cell periphery, leaving SHIP2 in the cytosol, following EGF stimulation (Fig. 5*G*). It was of interest that the amount of α-tubulin was also decreased in LL5β knockdown cells (Fig. 5*E*). Because it has been reported that SHIP2 regulates PtdIns(3,4,5)P_3 at membrane ruffles (14) and because it has also been proposed that SHIP2 mediates negative feedback on the accumulation of PtdIns(3,4,5)P_3 (13), we examined whether SHIP2, which is directed by LL5β through Filamin A, regulates membrane PtdIns(3,4,5)P_3. We found that ARNO-PH, one of the widely used PtdIns(3,4,5)P_3 detectors (16, 17) (supplemental Figs. S2 and S4 and supplemental Video 3), showed a greater accumulation at the plasma membrane in LL5β knockdown cells (Fig. 5, *H* and *I*). This suggests that SHIP2, which is directed by LL5β, is very likely to regulate membrane PtdIns(3,4,5)P_3.

DISCUSSION

We demonstrate here that LL5β is essential for quick Filamin A-dependent SHIP2 translocation in response to membrane PtdIns(3,4,5)P_3, fast enough to chase PtdIns(3,4,5)P_3 changes, and the reciprocal control of membrane PtdIns(3,4,5)P_3 through SHIP2, as well as the enhanced lamellipodium formation induced by PtdIns(3,4,5)P_3 (Fig. 6). It has been reported that v-ral simian leukemia viral oncogene homolog A (RalA) targets Filamin A in filopodia (22). In addition, faint membrane localization of mutated SHIP2 that lacks Filamin A-interacting domain, is observed after 5 min of EGF stimulation (14). This is consistent with the fact that SHIP2 is capable of associating with $p130^{Cas}$ and localizes to membrane ruffles and focal adhesions (23).

Because F-actin primarily grows near the plasma membrane by polymerizing globular actins at its plus end (24) and because cells do not form lamellipodia (large protrusions) in response to EGF application in the presence of the non-membrane-associating LL5βΔPH mutant, it is likely that increasing the cross-linking of newly polymerized F-actins by membrane-recruited Filamin A helps a cell to form lamellipodia. It is of interest that Filamin A can regulate the formation of small membrane protrusions without its actin-cross-linking activity. Indeed, small pseudopods were formed in M2 cells transfected with Filamin AΔABD in response to EGF.

LL5β, as well as Filamin A, is apparently versatile because the amount of α-tubulin in the membrane fraction was decreased by LL5β knockdown. It has been reported that LL5β binds to cytoplasmic linker-associated proteins (CLASPs) (25), which attach to the plus ends of microtubules, thereby modulating microtubule stabilization (26). Therefore, it is possible that LL5β synchronizes actins and microtubules, thereby coordinating cytoskeletal components for efficient migration.

It has been shown that SHIP2 is a critical component of a negative feedback loop that regulates PtdIns(3,4,5)P_3 levels and is likely to help a cell respond accurately and dynamically to external signals that impart directionality (13). We show here that SHIP2 translocates directly to sites of PtdIns(3,4,5)P_3 accumulation with Filamin A, which is dependent on LL5β. Considering that LL5β accumulates to the membrane in response to EGF application within a few minutes, it is plausible that SHIP2 follows changes in PtdIns(3,4,5)P_3 without a substantial delay. Therefore, it is likely that SHIP2, Filamin A, and LL5β help a cell to move in one direction smoothly. Moreover, the ability of PtdIns(3,4,5)P_3 and SHIP2 to regulate various cellular responses, such as the insulin response (27), and the reciprocal regulation of PtdIns(3,4,5)P_3 with Filamin A-LL5β reported here suggest that these findings are significant for the general understanding of such events, and possibly, for the understanding of related diseases.

Acknowledgments—We thank T. Bando, H. Yoshikawa, K. Hisazaki, and T. Taniguchi for technical and secretarial assistance and Y. Ohta, T. P. Stossel, and Y. Yokota for critical reading. We are also grateful to T. Sasaoka for discussions about SHIP2, Y. Ohta and T. P. Stossel for A7 and M2 cells, D. W. Chung for providing human Filamin C cDNA, J. Miyazaki for the pCAGGS vector, T. Balla for ARNO/PH, and J. Y. Yu and D. L. Turner for the mU6pro vector.

REFERENCES

1. Merlot, S., and Firtel, R. A. (2003) *J. Cell Sci.* **116,** 3471–3478
2. Franca-Koh, J., Kamimura, Y., and Devreotes, P. N. (2007) *Nat. Cell Biol.* **9,** 15–17
3. Gorlin, J. B., Yamin, R., Egan, S., Stewart, M., Stossel, T. P., Kwiatkowski, D. J., and Hartwig, J. H. (1990) *J. Cell Biol.* **111,** 1089–1105
4. Cunningham, C. C., Gorlin, J. B., Kwiatkowski, D. J., Hartwig, J. H., Janmey, P. A., Byers, H. R., and Stossel, T. P. (1992) *Science* **255,** 325–327
5. Takenawa, T., and Suetsugu, S. (2007) *Nat. Rev. Mol. Cell Biol.* **8,** 37–48
6. Harlan, J. E., Hajduk, P. J., Yoon, H. S., and Fesik, S. W. (1994) *Nature* **371,** 168–170
7. Lemmon, M. A., and Ferguson, K. M. (2000) *Biochem. J.* **350,** 1–18
8. Franke, T. F., Kaplan, D. R., Cantley, L. C., and Toker, A. (1997) *Science* **275,** 665–668
9. Itoh, T., and Takenawa, T. (2002) *Cell. Signal.* **14,** 733–743
10. Levi, L., Hanukoglu, I., Raikhinstein, M., Kohen, F., and Koch, Y. (1993) *Biochim. Biophys. Acta* **1216,** 342–344
11. Paranavitane, V., Coadwell, W. J., Eguinoa, A., Hawkins, P. T., and Stephens, L. (2003) *J. Biol. Chem.* **278,** 1328–1335
12. Paranavitane, V., Stephens, L. R., and Hawkins, P. T. (2007) *Cell. Signal.* **19,** 817–824
13. Aoki, K., Nakamura, T., Inoue, T., Meyer, T., and Matsuda, M. (2007) *J. Cell Biol.* **177,** 817–827
14. Dyson, J. M., O'Malley, C. J., Becanovic, J., Munday, A. D., Berndt, M. C., Coghill, I. D., Nandurkar, H. H., Ooms, L. M., and Mitchell, C. A. (2001) *J. Cell Biol.* **155,** 1065–1079
15. Nagano, T., Morikubo, S., and Sato, M. (2004) *J. Neurosci.* **24,** 9648–9657
16. Várnai, P., Bondeva, T., Tamás, P., Tóth, B., Buday, L., Hunyady, L., and Balla, T. (2005) *J. Cell Sci.* **118,** 4879–4888
17. Navolanic, P. M., Steelman, L. S., and McCubrey, J. A. (2003) *Int. J. Oncol.* **22,** 237–252
18. Klarlund, J. K., Tsiaras, W., Holik, J. J., Chawla, A., and Czech, M. P. (2000) *J. Biol. Chem.* **275,** 32816–32821
19. Oikawa, T., Yamaguchi, H., Itoh, T., Kato, M., Ijuin, T., Yamazaki, D., Suetsugu, S., and Takenawa, T. (2004) *Nat. Cell Biol.* **6,** 420–426
20. Stossel, T. P., Condeelis, J., Cooley, L., Hartwig, J. H., Noegel, A., Schleicher, M., and Shapiro, S. S. (2001) *Nat. Rev. Mol. Cell Biol.* **2,** 138–145
21. van der Flier, A., and Sonnenberg, A. (2001) *Biochim. Biophys. Acta* **1538,** 99–117
22. Ohta, Y., Suzuki, N., Nakamura, S., Hartwig, J. H., and Stossel, T. P. (1999)

Proc. Natl. Acad. Sci. U.S.A. **96,** 2122–2128
23. Prasad, N., Topping, R. S., and Decker, S. J. (2001) *Mol. Cell. Biol.* **21,** 1416–1428
24. Watanabe, N., and Mitchison, T. J. (2002) *Science* **295,** 1083–1086
25. Lee, H., Engel, U., Rusch, J., Scherrer, S., Sheard, K., and Van Vactor, D. (2004) *Neuron* **42,** 913–926
26. Lansbergen, G., Grigoriev, I., Mimori-Kiyosue, Y., Ohtsuka, T., Higa, S., Kitajima, I., Demmers, J., Galjart, N., Houtsmuller, A. B., Grosveld, F., and Akhmanova, A. (2006) *Dev. Cell* **11,** 21–32
27. Kagawa, S., Soeda, Y., Ishihara, H., Oya, T., Sasahara, M., Yaguchi, S., Oshita, R., Wada, T., Tsuneki, H., and Sasaoka, T. (2008) *Endocrinology* **149,** 642–650

Letter to the Editor

S2554X mutation in the filaggrin gene is associated with allergen sensitization in the Japanese population

To the Editor:

Atopic diseases such as atopic dermatitis (AD) and allergic rhinitis are some of the most common diseases in developed societies, and the number of patients with these diseases is increasing. These diseases are caused by interactions between genetic and environmental factors; some patients develop various atopic diseases concurrently, whereas others show a gradual progression from one manifestation of allergy to the next (atopic march),[1] thereby indicating common genetic/environmental features among atopic diseases.

Skin barrier dysfunction may contribute to the allergen penetration responsible for AD and predate the development of asthma and allergic rhinitis.[2] Filaggrin (filament-aggregating protein; FLG) has been reported to play an important role in skin-barrier formation and hydration. FLG aggregates the keratin cytoskeleton to facilitate the collapse and flattening of keratinocytes in the outermost skin layer. Null mutations in *FLG* are associated with AD in various populations, and some mutations showed associations with rhinitis and allergen sensitization in white pediatric populations.[3] In a recent study, *Flg*-deficient mice showed a predisposition to sensitization after percutaneous exposure to an allergen and developed cutaneous inflammatory infiltration and allergen-specific immune responses after allergen sensitization.[4] We previously reported that the null allele of *FLG* showed statistically significant association with AD, and this association was stronger in the Japanese patients with the only-AD phenotype—that is, patients with AD without other atopic diseases.[5] However, the effects of *FLG* null mutations on other atopic conditions have not been investigated in Asian populations. In the current study, we genotyped 4 *FLG* null mutations in the Japanese general population and studied the association between these mutations and atopic phenotypes.

Between 2003 and 2007, 1575 hospital workers and university students were invited to participate in this study. All the participants were of Japanese origin and were residents of Fukui prefecture, Japan. The characteristics of the study population are shown in Table I. Asthma was diagnosed on the basis of whether patients answered that they had ever been diagnosed with asthma by a doctor. Allergic rhinitis was diagnosed on the basis of a positive history of rhinitis during the pollen season and/or all seasons, and high levels of allergen-specific IgE antibodies in the serum (RAST score ≥class 2). Total and specific IgE (produced in response to Japanese cedar, *Dermatophagoides*, *Dactylis glomerata*, *Ambrosia artemisiifolia*, *Candida albicans*, and *Aspergillus*) were measured by using the CAP-RAST method (Pharmacia Diagnostics AB, Uppsala, Sweden), and positive allergic sensitization was defined if the levels of 1 or more specific IgE molecules were greater than or equal to 0.70 IU/mL (class2). All the participants gave their written informed consent to participate in the study. The study was approved by the ethical committees of the University of Tsukuba and the University of Fukui, Japan.

Genomic DNA was extracted from whole-blood samples by using a DNA-isolation kit (QuickGene-810^{R}; Fuji, Tokyo, Japan). The 3321delA genotype was determined by sizing a fluorescently labeled PCR fragment on an Applied Biosystems 3100 DNA Sequencer (Applied Biosystems, Foster City, Calif) as described previously.[6] S2554X, S2889X, and S3296X were genotyped on TaqMan Assay-by-Design system for single nucleotide polymorphism genotyping (Applied Biosystems). The accuracy of genotyping was confirmed by using direct sequences/restriction fragment length polymorphism analysis[7] of samples obtained from all carriers and selected noncarriers of the null mutations.

TABLE I. Characteristics of the study population (1499 subjects)

Sex (male:female)	**466:1033**
Age (y), mean ± SD	32.3 ± 9.7
Asthma (current and past)	104/1093
Allergic rhinitis	575/1093
Sensitization	1014/1499
Total IgE (IU/mL), geometric mean	65.6 (range, <5-24,000)
Specific IgE (U_A/mL),	**Prevalence (range, U_A/mL)**
Mite	39% (<0.34-100)
Japanese cedar	62% (<0.34-100)
Dactylis glomerata	26% (<0.34-100)
Ambrosia artemisiifolia	12% (<0.34-32)
Candida albicans	6.5% (<0.34-35.8)
Aspergillus	3.3% (<.034-9.1)

Total IgE values of <5 IU/mL have been considered as 0.1 IU/mL for the sake of calculations. The prevalence of specific IgE was calculated as the proportion of subjects with specific IgE titer of >0.70 U_A/mL.

The genetic effects of the association between the case-control status and each individual single nucleotide polymorphism were estimated by logistic regression analysis after adjusting for sex and age; the analysis was performed by using R version 2.7.0 (http://www.r-project.org/). The Fisher exact test was applied when the genotype counts were 0 and logistic regression could not be performed.

Among the 1575 participants, we obtained DNA samples and information on total and specific IgE levels for 1499 participants. Among these, 1093 subjects completed the asthma/rhinitis questionnaire, whereas 98 subjects (6.5%) had at least 1 *FLG* null mutation, and 1 subject was a combined heterozygote for null mutations. There was no deviation from the Hardy-Weinberg equilibrium ($P > .05$). The results of the association study are shown in Table II. *FLG* mutations were not associated with asthma and allergic rhinitis ($P > .05$). However, allergen sensitization was more common in the S2554X carriers ($P = .013$), and the trend toward association was observed in the 3321delA carriers ($P = .078$). However, the more common null mutation, S2889X, was not associated with allergen sensitization ($P > .05$), resulting in the disappearance of the association in the combined results ($P > .05$).

This is the first population-based study on the effects of *FLG* null mutations in the atopic phenotypes in Asian populations, and specific null mutations were found to be associated with allergen sensitization. In large population-based studies, a detailed clinical diagnosis of asthma and rhinitis cannot be easily performed, and careful examination of the subjects can yield stronger

TABLE II. Results of association study with atopic phenotypes in 98 subjects with filaggrin null mutations

Phenotype	AA	Aa	aa	*P* value	OR (95% CI)
Asthma/without asthma					
3321delA	104/976	0/13	0/0	.98	NA
S2554X	104/980	0/9	0/0	.98	NA
S2889X	99/947	5/42	0/0	.86	1.09 (0.42-2.85)
S3296X	104/980	0/9	0/0	.98	NA
Combined	99/917	5/71	0/1	.36	0.65 (0.25-1.65)
Allergic rhinitis/without allergic rhinitis					
3321delA	567/513	8/5	0/0	.53	1.43 (0.46-4.41)
S2554X	569/515	6/3	0/0	.37	1.89 (0.47-7.61)
S2889X	552/494	23/24	0/0	.60	0.85 (0.48-1.54)
S3296X	571/513	4/5	0/0	.61	0.70 (0.18-2.66)
Combined	535/481	39/37	1/0	.90	0.97 (0.61-1.55)
Sensitization/without sensitization					
3321delA	1000/483	14/2	0/0	.078	3.81 (0.86-16.89)
S2554X	1001/485	13/0	0/0	.013	NA
S2889X	977/467	37/18	0/0	.99	0.99 (0.56-1.77)
S3296X	1004/480	10/5	0/0	.94	0.96 (0.32-2.85)
Combined	941/460	72/25	1/0	.11	1.47 (0.91-2.35)

AA, Wild-type for the mutation; *Aa*, heterozygote for the mutation; *aa*, homozygote for the mutation or a compound heterozygote for mutations; *NA*, not applicable; *OR*, odds ratio. Q10
The number of subjects with a particular genotype is represented in the following form: number of subjects with the phenotype (eg, asthma)/number of subjects without the phenotype (eg, asthma).

estimates of associations. Allergic rhinitis showed high prevalence in the subjects in this study; nearly half of the subjects were affected. This is a result of the high prevalence (31.4% to 39.1%) of Japanese cedar pollinosis among adults age 20 to 49 years.[8]

The reason for the association between specific null mutations and allergen sensitization remains to be determined, but our AD case-control samples also showed a similar trend; the odds ratios for the development of AD were 5.0 in the case of S2554X and 2.27 in the case of S2889X (see this article's Methods and Table E1 in the Online Repository at www.jacionline.org). Similar trends were also observed in white populations.[9] *FLG* consists of 10 to 13 *FLG* tandem homologous sequence units, and each null mutation is linked to a particular *FLG* homologous unit. Therefore, we speculated that the effects of *FLG* null mutations vary according to their locations and units.

The current study has a number of limitations. In a majority of the subjects with *FLG* null mutations, the mutations did not show an association with allergen sensitization. Furthermore, our study population contained only a small number of subjects with S2554X null mutations. In addition, the lack of independent general populations for use in replication analysis may weaken our observations. Future studies should aim to identify the precise mechanisms of *FLG* null mutations in the development of atopic phenotypes.

Yoshimasa Imoto, MD[a,d]
Hisako Enomoto, MD, PhD[a,b]
Shigeharu Fujieda, MD, PhD[d]
Masayuki Okamoto[d]
Masafumi Sakashita[d]
Q4
Dai Susuki[d]
Masafumi Okada, MD, PhD[c]
Tomomitsu Hirotac[c]
Mayumi Tamaric[c]
Kouji Ebed[f]
Tadao Arinami, MD, PhD[a]
Emiko Noguchi, MD, PhD[a]

From the Departments of [a]Medical Genetics, [b]Dermatology, and [c]Epidemiology, Graduate School of Comprehensive Human Sciences, University of Tsukuba; [d]the Departments of Otorhinolaryngology and Immunology, University of Fukui Faculty of Medical Sciences; [e]the Laboratory of Genetics of lung disease, RIKEN Single Nucleotide Polymorphism Research Center, Yokohama; and [f]Takao Hospital, Kyoto, Japan. E-mail: enoguchi@md.tsukuba.ac.jp

Supported by Grants-in-Aid for Scientific Research from the Ministry of Health and Welfare, Japan (H17-Genome-001, H17-Immunology-001, H20-Immunology-001, -004) and from the Ministry of Education, Science and Culture of Japan (17390458, 18591097, 20390441).

Disclosure of potential conflict of interest: The authors have declared that they have no conflict of interest.

REFERENCES

1. Linneberg A. The allergic march in early childhood and beyond. Clin Exp Allergy 2008;38:1419-21.
2. Proksch E, Folster-Holst R, Jensen JM. Skin barrier function, epidermal proliferation and differentiation in eczema. J Dermatol Sci 2006;43:159-69.
3. Henderson J, Northstone K, Lee SP, Liao H, Zhao Y, Pembrey M, et al. The burden of disease associated with filaggrin mutations: a population-based, longitudinal birth cohort study. J Allergy Clin Immunol 2008;121:872-7. Q5
4. Fallon PG, Sasaki T, Sandilands A, Campbell LE, Saunders SP, Mangan NE, et al. A homozygous frameshift mutation in the mouse Flg gene facilitates enhanced percutaneous allergen priming. Nat Genet 2009;41:602-8.
5. Enomoto H, Hirata K, Otsuka K, Kawai T, Takahashi T, Hirota T, et al. Filaggrin null mutations are associated with atopic dermatitis and elevated levels of IgE in the Japanese population: a family and case-control study. J Hum Genet 2008;53:615-21.
6. Nomura T, Sandilands A, Akiyama M, Liao H, Evans AT, Sakai K, et al. Unique mutations in the filaggrin gene in Japanese patients with ichthyosis vulgaris and atopic dermatitis. J Allergy Clin Immunol 2007;119:434-40.
7. Nomura T, Akiyama M, Sandilands A, Nemoto-Hasebe I, Sakai K, Nagasaki A, et al. Specific filaggrin mutations cause ichthyosis vulgaris and are significantly associated with atopic dermatitis in Japan. J Invest Dermatol 2008;128:1436-41.
8. Baba K. Guideline for nasal allergy practice. Life Sci 2009. Q6
9. Sandilands A, Terron-Kwiatkowski A, Hull PR, O'Regan GM, Clayton TH, Watson RM, et al. Comprehensive analysis of the gene encoding filaggrin uncovers prevalent and rare mutations in ichthyosis vulgaris and atopic eczema. Nat Genet 2007;39:650-4.

doi:10.1016/j.jaci.2009.10.062

METHODS

Subjects

For a case-control study of AD, 376 independent patients with AD (age 16-64 years; mean, 29.7 years) were recruited. AD was diagnosed in subjects according to the criteria of Hanifin and Rajka.[E1] All patients had pruritus, a typical appearance of AD, and a tendency toward chronic or chronically relapsing dermatitis. Control subjects for the case-control study were 923 healthy adults (age 19-78 years; mean, 46.2 years) with no history of any allergic disease. The subjects were the same in our previous study.[E2] A full verbal and written explanation of the study was given to patients and controls, and subjects who gave informed consent participated in this study. This study was approved by the Committee of Ethics of the University of Tsukuba.

Genotyping of *FLG* null mutations

Genomic DNA was extracted from whole-blood samples by using a DNA-isolation kit (QuickGene-810R; Fuji, Tokyo, Japan). The 3321delA genotype was determined by sizing a fluorescently labeled PCR fragment on an Applied Biosystems 3100 DNA Sequencer (Applied Biosystems, Foster City, Calif) as described previously.[E3] S2554X, S2889X, and S3296X were genotyped on a TaqMan Assay-by-Design system for single nucleotide polymorphism genotyping (Applied Biosystems). The accuracy of genotyping was confirmed by using direct sequences/restriction fragment length polymorphism analysis[E4] of samples obtained from all carriers and selected noncarriers of the FLG QJ1 null mutations.

REFERENCES

E1. Hanifin J, Rajka G. Diagnostic feature of atopic dermatitis. Acta Derm Venereol 1980:(suppl 92):44-7. QJ2
E2. Enomoto H, Hirata K, Otsuka K, Kawai T, Takahashi T, Hirota T, et al. Filaggrin null mutations are associated with atopic dermatitis and elevated levels of IgE in the Japanese population: a family and case-control study. J Hum Genet 2008:53: 615-21.
E3. Nomura T, Sandilands A, Akiyama M, Liao H, Evans AT, Sakai K, et al. Unique mutations in the filaggrin gene in Japanese patients with ichthyosis vulgaris and atopic dermatitis. J Allergy Clin Immunol 2007:119:434-40.
E4. Nomura T, Akiyama M, Sandilands A, Nemoto-Hasebe I, Sakai K, Nagasaki A, et al. Specific filaggrin mutations cause ichthyosis vulgaris and are significantly associated with atopic dermatitis in Japan. J Invest Dermatol 2008:128:1436-41.

TABLE E1. AD case-control study

Polymorphism	Population*	Genotyped (%)	Genotype count (frequency, %)						Genotypic *P* value*	Allelic *P* value†	Odds ratio (95% CI)‡
			AA		Aa		aa				
3321delA	AD	97.3	356	(97.3)	10	(2.7)	0	(0)	.077	.079	2.1 (0.9-4.9)
	Controls	99	902	(98.7)	12	(1.3)	0	(0)			
			AA		Aa		aa				
S2554X*	AD	99.7	365	(97.3)	10	(2.7)	0	(0)	.0012	.0012	5.0 (1.7-14.8)
	Controls	100	918	(99.5)	5	(0.5)	0	(0)			
			AA		Aa		aa				
S2889X	AD	97.6	346	(94.3)	21	(5.7)	0	(0)	.0058	.0063	2.27 (1.25-4.14)
	Controls	100	899	(97.0)	24	(3.0)	0	(0)			
			AA		Aa		aa				
S3296X	AD	98.7	369	(99.5)	2	(0.5)	0	(0)	.82	.82	0.83 (0.17-4.12)
	Controls	100	917	(99.3)	6	(0.7)	0	(0)			
Combined			AA		Aa		aa				
(4 null mutations)	AD	93.4	308	(87.7)	43	(12.3)	0	(0)	.000011	.000016	2.57 (1.67-3.97)
	Controls	99	867	(94.9)	47	(5.1)	0	(0)			

AA, Wild-type for the mutation; *Aa*, heterozygote for the mutation; *aa*, homozygote for the mutation or a compound heterozygote for mutations.
*Genotypic *P* value was calculated with χ^2 test in comparison with wild-type homozygote versus minor allele heterozygote plus minor allele homozygote.
†Allelic *P* values were calculated with χ^2 test in comparison with genotype and allele counts in controls, respectively.
‡Odds ratio for the wild-type homozygote versus minor allele heterozygote and minor allele homozygote.

Cytokine xxx (2010) xxx–xxx

Contents lists available at ScienceDirect

Cytokine

journal homepage: www.elsevier.com/locate/issn/10434666

Poly(I:C) induces BLyS-expression of airway fibroblasts through phosphatidylinositol 3-kinase

Takechiyo Yamada *, Su Lizhong, Noboru Takahashi, Seita Kubo, Norihiko Narita, Dai Suzuki, Tetsuji Takabayashi, Yuichi Kimura, Shigeharu Fujieda

Department of Otorhinolaryngology, University of Fukui, Fukui 910-1193, Japan

ARTICLE INFO

Article history:
Received 22 September 2009
Received in revised form 5 November 2009
Accepted 17 December 2009
Available online xxxx

Keywords:
BLyS
Fibroblast
Airway
dsRNA
PI3K

ABSTRACT

B lymphocyte stimulator (BLyS), B cell activating factor (BAFF), a member of the tumor necrosis factor ligand superfamily has potent co-stimulatory activity on B cells, and BLyS-production in the airway mucosa is of potential importance as it triggers innate and adaptive immune responses. To investigate whether airway fibroblast could express BLyS, we examined BLyS-expression in human nasal airway fibroblasts and compared to its expression in tonsillar and skin fibroblasts as well as the effect of the Toll-like receptor (TLR) ligands on that in human nasal airway fibroblasts. The expression of BLyS by nasal fibroblasts in the presence of polyinocinic–polycytidykic acid (poly(I:C)) was markedly induced, to a level of more than 100 times higher than that observed in the absence of poly(I:C). In order to demonstrate the intracellular pathways involved in poly(I:C)-induced BLyS-expression, we used specific inhibitors of phosphatidylinositol 3-kinase (PI3-kinase), spleen tyrosine kinase (Syk), p38 mitogen-activated protein kinase (p38 MAPK), c-Jun N-terminal kinase (JNK), and extracellular-signal related kinase (ERK)-signaling in these events. Pre-incubation with the PI3-kinase inhibitor LY294002 or Wortmanin reversed the poly(I:C)-induced production and expression of BLyS. Syk kinase inhibitor Piceatannol partially reduced its production and expression. Thus, we were able to show that PI3-kinase signaling is directly involved in poly(I:C)-induced BLyS-expression in nasal airway fibroblasts. These results indicate that human nasal airway fibroblasts strongly induce BLyS-expression and production by poly(I:C) through PI3-K signaling during airway immune responses.

1. Introduction

TNF ligand superfamily member 13B, BLyS,[1] BAFF, plays critical roles in respiratory mucosal defense, because it is a potent co-activator of B cells in vitro or in vivo. BLyS induces B cell proliferation, human Ig class switch recombination, and Ig secretion [1–3]. Activation of B cells in the airways is now believed to be of great importance in immunity to pathogens, and it also participates in the pathogenesis of airway diseases. The expression of BLyS was detected in TLR ligand-treated BEAS-2B cells and primary human bronchial epithelial cells [4]. In the nasal mucosa, the expression of BLyS for in sinonasal tissue was found to be significantly correlated with CD20, and overproduction of BLyS contributes to the pathogenesis of chronic rhinosinusitis via the local induction of IgA and the activation of eosinophils [5]. Although nasal airway fibroblasts are a rich source of cytokines, chemokines, and growth factors, it is unknown whether airway fibroblast could express BLyS.

As 'a mucosal guardian' in the upper airway, the inferior turbinate of the human nose is easily exposed to a variety of stimulus such as viral and bacterial infection during the common cold. Most of the viruses that cause upper respiratory infection are RNA viruses including rhinoviruses, coxsackievirus, echovirus, and influenza viruses. RNA viruses synthesize double-stranded RNA (dsRNA) during replication [6], and this is a strong stimulus for innate anti-viral responses through the secretion of cytokines. TLRs play key roles in innate immunity by recognizing microbial conserved pathogen-associated molecular patterns, and TLR3 is involved in the recognition of the synthetic dsRNA analogue, polyinocinic–polycytidykic acid (polyI:C) [7]. It is not clear which TLR ligand induces BLyS-expression or production of human airway fibroblasts.

* Corresponding author. Address: Department of Otorhinolaryngology, University of Fukui, 23-3 Matsuoka-Shimoaizuki, Eiheiji, Yoshida, Fukui 910-1193, Japan. Tel.: +81 776 61 8407; fax: +81 776 61 8118.
E-mail address: ymdtkcy@u-fukui.ac.jp (T. Yamada).

[1] *Abbreviations used:* BLyS, B lymphocyte stimulator; BAFF, B cell activating factor; TLR, Toll-like receptor; dsRNA, double-stranded RNA; IRF, interferon regulatory factor; PGN, peptidoglycan; poly(I:C), polyinocinic-polycytidykic acid; LPS, Lipopolysaccharide; PI-3K, phosphatidylinositol 3-kinase; Syk, spleen tyrosine kinase; JNK, c-Jun N-terminal kinase; p38 MAPK, p38 mitogen-activated protein kinase; JNK, c-Jun N-terminal kinase; ERK, extracellular-signal related kinase; TACI, transmembrane activator and CAML interactor.

1043-4666/$ - see front matter Crown Copyright © 2010 Published by Elsevier Ltd. All rights reserved.
doi:10.1016/j.cyto.2009.12.011

Please cite this article in press as: Yamada T et al. Poly(I:C) induces BLyS-expression of airway fibroblasts through phosphatidylinositol 3-kinase. Cytokine (2010), doi:10.1016/j.cyto.2009.12.011

The presence of dsRNA during viral infections is a key step in the activation of several signaling pathways, including mitogen-activated protein kinase (MAPK), activator protein-1, and interferon regulatory factors (IRFs). Poly(I:C) induces the rapid activation of the mitogen-activated protein kinases (MAPKs) (p38 MAPK, c-Jun N-terminal kinase (JNK), ERK) and MAPK-dependent expression of proinflammatory cytokines, chemokines, and adhesion molecules [8,9]. In accordance with the expression of TLR3, poly(I:C) stimulation induces the activation of interferon regulatory factor-3 (IRF-3) transcription factor and p38 MAPK [10]. PI3-kinase plays an essential role in IRF-3-binding to the promoter of the target gene and TLR3-mediated gene induction by dsRNA-treated cells [11]. Spleen tyrosine kinase (Syk) regulates PI3K activation and RNA virus endocytosis in the airway mucosae [12]. The potential role of dsRNA-induced BLyS-expression in signaling is poorly understood.

Although the ability of BLyS-production from airway mucosa is of potential importance as it provides innate and adaptive immune responses, the details of BLyS-expresion in airway fibroblasts remains unexplored. In this study, we established fibroblast lines from the human inferior turbinate and other tissues, and it has been confirmed whether BLyS is expressed in human nasal airway fibroblasts, tonsillar, and skin fibroblasts. We examined the effect on BLyS-expression of TLR ligands including peptidoglycan (PGN); poly(I:C); lipopolysaccharide (LPS); and CpG in human nasal airway fibroblasts. In order to demonstrate the intracellular pathways involved in dsRNA-induced BLyS-expression, we used specific inhibitors of PI3-kinase, Syk, p38 MAPK, JNK, and extracellular-signal related kinase (ERK)-signaling in these events.

2. Materials and methods

2.1. Reagents

The following reagents were used: poly(I:C) (Amersham Bioscience, Piscataway, NJ); PGN (Sigma); LPS (MERCK bioscience, Germany); CpG, a synthetic oligodeoxynucleotide that contains CpG motifs that mimicks bacterial DNA (5′-ACCGATCGTTCGGCCGGTGACGGCACCA-3′); SP600125 as a specific inhibitor of JNK (BIOMOL); SB203580 as a specific inhibitor of p38 MAP kinase (Promega); PD98059 as a specific inhibitor of MEK-1 (Promega); LY294002 as a specific inhibitor of PI3-kinase (Promega); Wortmannin (Sigma); AKT inhibitor (CALBIOCHEM); anti-human BLyS monoclonal Ab (R&D system); p44/42 MAP Kinase rabbit polyclonal antibody (Ab) (Cell Signaling, Beverly, MA); SAPK/JNK rabbit polyclonal Ab (Cell Signaling); phospho-p44/42 MAPK (E10) mouse monoclonal Ab (Cell Signaling); phospho-JNK (G9) mouse monoclonal Ab (Cell Signaling); phospho-p38 MAPK (28B10) mouse monoclonal Ab (Cell Signaling); phospho-AKT (587F11) mouse monoclonal Ab (Cell Signaling); AKT Rabbit polyclonal Ab (Cell Signaling); and p38 (A12) mouse monoclonal Ab (Santa Cruz Biotechnology, Santa Cruz, CA).

2.2. Cells, cell lines, and cell culture

Human primary nasal fibroblast lines were established from human nasal biopsy tissues of inferior turbinates removed during the operation ($n = 6$). All the nasal specimens had been taken from patients with allergic rhinitis. Five males and one female aged 30.5 ± 6.6 year (mean ± SEM) were atopic, diagnosed on the basis of elevation of at least one of the capsulated hydrophobic carrier polymer-radioallergosorbent tests against 8 common aeroallergens. All of the patients had a house dust or a cedar pollen CAP-RAST score of 2 or more. The subjects had given written informed consent, and its study protocol was approved by the Ethics Committee at University of Fukui. The patients had no smoking and no special background including pollution, without any medication at least 14 days before operation. Only fibroblast lines between the sixth and tenth passages were used in this study. No contamination of epithelial cells was confirmed by immunohistochemical examination using cytokeratin markers. The fibroblasts were stimulated by TLR ligands in RPMI-1640 medium supplemented with 10% FCS and in humidified atmosphere of 10% CO_2 in air at 37 °C.

2.3. Real time PCR

Total RNA was extracted using a total RNA isolation NucleoSpin™ RNA II Kit (MACHERY-NAGEL, Düren Germany). The reverse transcription reaction was performed with TaqMan® RT Reagents (Applied Biosystems Japan, Tokyo, Japan) using random hexamer primers. The amplification of TLRs, BLyS, and β_2-microglobulin-cDNA was performed in a MicroAmp optical 96-well reaction plate (Applied Biosystems). All TaqMan® probe/primer combinations used in this study were TaqMan® Gene Expression Assay products purchased from Applied Biosystems. β2-Microglobulin was chosen as the reference housekeeping gene because it is convenient to assay and highly expressed. Furthermore, in order to select the housekeeping gene, we evaluated it using a TaqMan® Human Endogenous Control Plate, which was most suitable. TaqMan® PCR was performed in a 20-μl volume using TaqMan® Universal PCR master mix (Applied Biosystems). The reaction was performed in an ABI PRISM 7000 Sequence Detection System (Applied Biosystems). The reaction mixtures were pre-incubated for 2 min at 50 °C. The PCR program involved 10 min of Taq Gold activation at 95 °C, followed by 40 cycles of 15 s at 95 °C and 1 min at 60 °C (maximum ramping speed between temperatures). Human cDNA equivalent to 50 ng of total RNA from each sample was assayed in each tube. The threshold cycle number was determined with sequence Detector Software (version 1.1: Applied Biosystems) and transformed using comparative methods as described by the manufacturer with β_2-microglobulin as the reference gene.

2.4. Cytokine assay

The cells were cultured in the presence of poly(I:C) for appropriate periods, and then the culture supernatants were harvested and stored at −80 °C. The amounts of BLyS in the cell culture supernatant were measured with an ELISA kit that was purchased from R&D system.

2.5. Immunoblot analysis

The samples were added to a 2-fold volume of sample buffer [95% laemmli sample buffer (BIORAD) and 5% 2-mercaptoethanol]. After heating the mixture at 95 °C for 5 min, the samples were electrophoresed. The proteins were then transferred electrophoretically onto polyvinylamidedifluoride membranes (Amersham Bioscience). The blotted membranes were rinsed with 5% non-fat-dried milk diluted in PBS containing 0.1% Tween 20 for 60 min at room temperature, and then incubated with the antibodies for 16 h at 4 °C. After being washed, the membranes were treated with HRP-conjugated anti-mouse immunoglobulin (Ig) Ab or HRP anti-rabbit Ig Ab (DAKO, Carpinteria, CA) for 60 min at room temperature. Peroxidase color visualization was achieved with TMB membrane peroxidase substrate (KPL, Gaithersburg, MD).

2.6. Antibody array

Signal Transduction AntibodyArray™ which contains 400 high quality antibodies against well-studied signaling proteins, was purchased from Proteomics Company. Nasal fibroblasts were stim-

Please cite this article in press as: Yamada T et al. Poly(I:C) induces BLyS-expression of airway fibroblasts through phosphatidylinositol 3-kinase. Cytokine (2010), doi:10.1016/j.cyto.2009.12.011

ulated with 10 μg/ml poly(I:C) for 30 min, washed twice with ice cold Tris saline (50 mM Tris pH 7.5, 150 mM NaCl, 1.5 mM PMSF), and lysed using Triton Extraction buffer containing 15 mM Tris pH 7.5, 120 mM NaCl, 25 mM KCl, 2 mM EGTA, 2 mM EDTA, 0.1 mM DTT, 0.5% triton X-100, 10 μg/ml leupeptin, and 0.5 mM PMSF. Pelleted cellular debris was removed by centrifugation at maximum speed (14,000 rpm). The supernatant was collected, and the membrane of Signal Transduction Antibody Array™ was incubated with the whole cell extracts in 5 ml extraction solution containing 1% BSA for 2 h at room temperature with slow shaking. After washing the membrane, HRP-conjugated anti phosphotyrosine antibody was applied for 2 h at room temperature. Peroxidase substrate was used and the membrane was washed and then exposed to X-ray film.

2.7. Data and statistical analysis

Statistical analysis was performed using the Wilcoxon signed-ranks test to assess the significance of differences.

3. Results

3.1. BLyS-expression in human fibroblasts

To determine whether BLyS is expressed in human fibroblasts, we established fibroblast lines from small pieces of human inferior turbinate, tonsil, and skin respectively from six individuals and then examined BLyS-expression in stimulated fibroblasts. As shown in Fig. 1, the expression of BLyS in nasal fibroblasts was markedly induced in the presence of poly(I:C), to a level more than 100 times higher than that observed in the absence of poly(I:C). In skin fibroblasts, we could not detect any induction of BLyS-expression in the presence of poly(I:C). Although poly(I:C) induced BLyS-expression by tonsillar fibroblasts, its induction was lower than that induced in nasal stimulated fibroblasts .

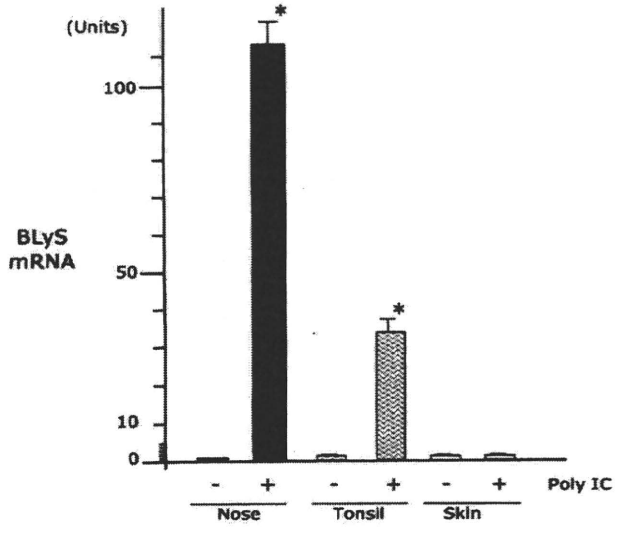

Fig. 1. BLyS-expression in human fibroblasts. After the cells has been treated with poly(I:C) (20 μg/ml) for 6 h, total RNA was isolated from human nasal (closed bar), tonsillar (waved bar), and skin (open bar) fibroblasts. The expression levels of BLyS-mRNA were assayed by real time RT-PCR. The RNA was reverse transcribed to cDNA, which was then used for real time PCR. Reactions were performed in three wells, and results are expressed relative to the expression levels of β_2-microglobulin. Data are expressed as the mean ± SEM of the fold increase relative to the control ($n = 6$). *$P < 0.05$ compared with control using Wilcoxon's signed-ranks test.

3.2. Toll-like receptor ligands and BLyS-expression

Since TLR 3 ligand strongly induced the expression of BLyS especially in human nasal fibroblasts, next we observed the expression of TLRs on human nasal fibroblasts. The mRNA expression of TLRs on fibroblasts was confirmed by real time RT-PCR. Fig. 2A shows the relative expression levels of TLR mRNAs on the cells. TLR 3 and 4 were highly expressed, while TLR 2 and 9 were moderately expressed. TLR1, 5, and 6 were also detected, but their expression levels were lower than those of TLR2, 3, 4, and 9. We could not detect the expression of TLR 7, 8, and 10 in human nasal fibroblasts. In order to look at which TLR ligand induces BLyS-expression in human nasal fibroblasts, we examined the effect on BLyS-expression of TLR ligands (PGN, poly(I:C), LPS, and CpG). Fibroblasts were treated with the agonists for 6 h, and BLyS-mRNA expression was assessed by real time PCR. The BLyS-expression was induced 100-fold by poly(I:C) and 10-fold ($P < 0.05$) by LPS in nasal fibroblasts, while it was hard to find any effecet by PGN or CpG on the level of mRNA for BLyS.

3.3. Dose-dependence and time-course of poly(I:C)-induced BLyS-expression

Having shown that TLR3 ligands strongly induce BLyS-expression in human nasal fibroblasts, next we have investigated its expression precisely. Poly(I:C) induced BLyS-mRNA expression in a dose-dependent manner with the maximal stimulation generally being at 10 μg/ml or higher, and its expression was detected 10-fold ($P < 0.05$) at 1 μg/ml in nasal fibroblasts (Fig. 3A). The exposure of nasal fibroblasts to TLR3 ligand triggered a rapid expression of BLyS-mRNA at 6 h and decreased thereafter. The expression was sustained at 80-fold at 24 h and 15-fold ($P < 0.05$) at 48 h (Fig. 3B).

3.4. Poly(I:C) induces BLyS-production from human nasal fibroblasts

Similar to other TNF family members, BLyS is generally expressed as a transmembrane protein and is cleaved from the surface to release its active soluble form. Production of soluble BLyS-proteins was detected using ELISA. Poly(I:C) increased BLyS-production at 1 μg/ml and higher ($P < 0.05$) in a dose-dependent manner (Fig. 4A) . Its production was 100 times higher than that detected in the absence of poly(I:C) at 10 μg/ml. Although the BLyS gene encodes a putative 285 amino acid (aa) type II transmembrane protein, the 152 aa form can also be shed from the membrane because the N-terminal side contains a furin cleavage site. We also examined the supernatants from human nasal fibroblasts using Western blotting. Fig. 4B shows that the soluble form of BLyS from human nasal fibroblast weighs 18 kDa, and its production occurred in a dose-dependent manner with the maximal stimulation observed at 10 μg/ml.

In the presence of IL-4, Ig class switch recombination in human B cells was always detected by BLyS-treatment at 100 ng/ml or higher [2]. The human nasal fibroblasts produce enough amounts of BLyS-protein to cause Ig class switch recombination, as shown in Fig. 4.

3.5. Suppression of poly(I:C)-induced and BLyS-production and expression by PI3-kinase inhibitor

Poly(I:C) is a TLR3 ligand that induces TLR3-signaling. We screened the intracellular signal transduction molecules of poly(I:C)-stimulated human nasal fibroblasts using *AntibodyArray™* which contains 400 high quality antibodies, and found that poly(I:C)-induced signaling involved Syk, Rho, or TRAF6. Also, we demonstrated that the exposure of cells to poly(I:C) triggered phosphorylation and activation of p38 MAPK, JNK, and AKT by

Please cite this article in press as: Yamada T et al. Poly(I:C) induces BLyS-expression of airway fibroblasts through phosphatidylinositol 3-kinase. Cytokine (2010), doi:10.1016/j.cyto.2009.12.011

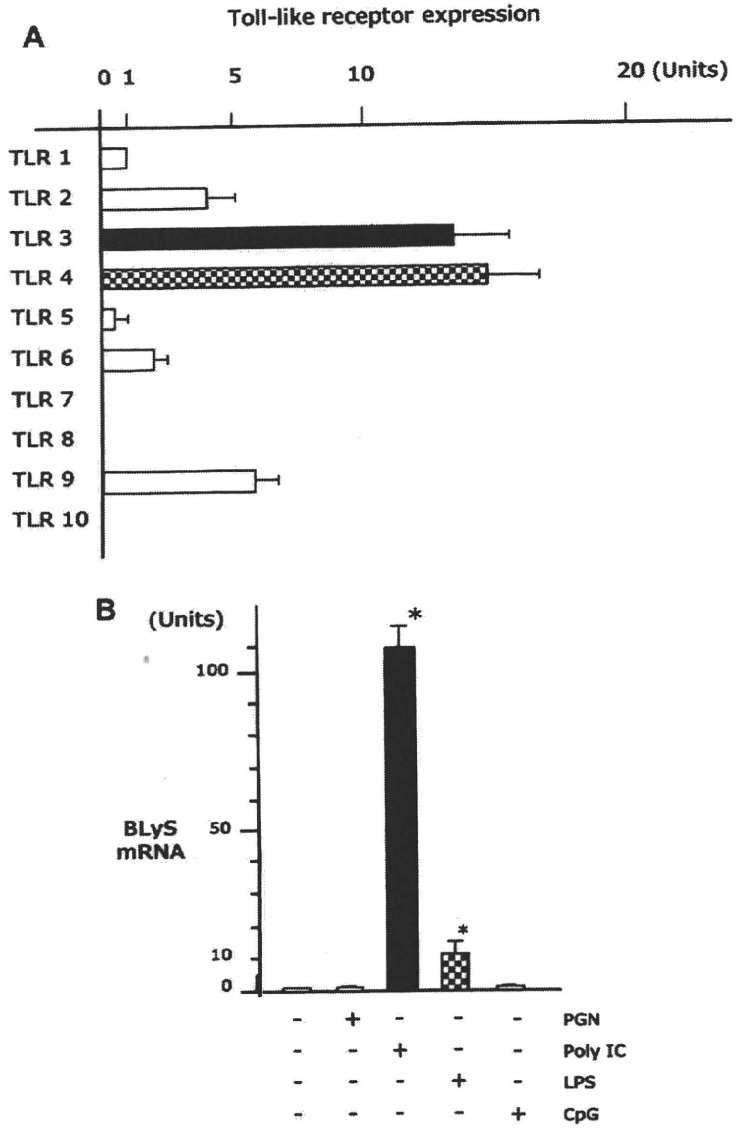

Fig. 2. Toll-like receptor ligands and BLyS-expression. (A) TLR1–9 mRNA expression levels were assayed by real time RT-PCR using a cDNA template derived from human nasal fibroblasts. The results are expressed relative to the expression levels of β_2-microglobulin ($n = 6$). (B) Analysis of the expression of BLyS-mRNA induced by Toll-like receptor ligands using real time PCR. Fibroblasts were treated with PGN (20 μg/ml), poly(I:C) (20 μg/ml), LPS (1 μg/ml), or CpG (1 μM) for 6 h. The RNA was isolated from the cells and BLyS-expression was measured. Data are expressed as the mean ± SEM of the fold increase relative to the control ($n = 6$). *$P < 0.05$.

Western blotting with specific antibodies to phosphorylated p38 MAPK, JNK, and AKT. Since PI3-kinase participates in TLR3-signaling [11], we sought to determine whether MAPKs, Syk kinase, or PI3-kinase signaling is directly involved in BLyS-expression. To accomplish this, we tested the ability of SB203580 (a specific inhibitor of p38 MAPK signaling), SP600125 (JNK inhibitor), PD98059 (a specific inhibitor of ERK signaling), Piceatannol (an inhibitor of Syk kinase), LY294002 and Wortmanin (PI3-kinase inhibitor) to affect the expression of BLyS in nasal fibroblasts stimulated with poly(I:C) (Figs. 5 and 6A).

Pre-incubation with the PI3-kinase inhibitor LY294002 and Wortmanin markedly suppressed the poly(I:C)-induced production and expression of BLyS, although inhibition of p38 MAP, JNK, and ERK did not have any effect. The Syk kinase inhibitor Piceatannol reduced poly(I:C)-induced production and expression of BLyS by 40% (Figs. 5 and 6A). The specific PI3-kinase inhibitor LY294002 reversed its expression in a dose-dependent manner (Fig. 6B). LY294002 decreased the expression of BLyS in poly(I:C)-stimulated nasal fibroblasts by 90% compared to the control level ($P < 0.05$). There were no differences in cell shape or viability among the four inhibitors.

4. Discussion

In the present study, we demonstrated that the expression of BLyS was strongly induced by nasal airway fibroblasts in the presence of poly(I:C), while we could not detect any induction of BLyS-expression in skin fibroblasts. Consistent with the high expression of TLR 3 and 4 mRNA on nasal airway fibroblasts, poly(I:C) and LPS induced BLyS-expression. Poly(I:C) induced BLyS-mRNA expression and protein-production in a dose-dependent manner. BLyS-expression and production from airway fibroblasts has not been reported previously, although BLyS is expressed in proinflammatory-cytokine-stimulated fibroblast-like synoviocytes from the inflamed

Please cite this article in press as: Yamada T et al. Poly(I:C) induces BLyS-expression of airway fibroblasts through phosphatidylinositol 3-kinase. Cytokine (2010), doi:10.1016/j.cyto.2009.12.011